An Alternative Scheme for Chiron Fiber and Slicer Mode Data Reductions

Frederick M. Walter
Stony Brook University
27 September 2017
update: 7 February 2018

Chiron (Tokovinin et al. 2012) is a stable high-throughput bench-mounted echelle spectrograph fed by the 1.5m telescope on Cerro Tololo, operated by the SMARTS partnership. Three years of experience with *Chiron*, observing types of objects that *Chiron* was never designed to observed, have revealed some deficiencies in the standard data processing. I discuss here a new data reduction scheme for data obtained in the fiber and slicer modes. This provides different treatments of the local background and cosmic ray rejection, permits Gaussian extractions in addition to boxcar extractions, extracts 13 additional orders (down to about 4085Å), and provides more order overlap and flatter orders. This may enable new and different kinds of science from the *Chiron* spectrograph.

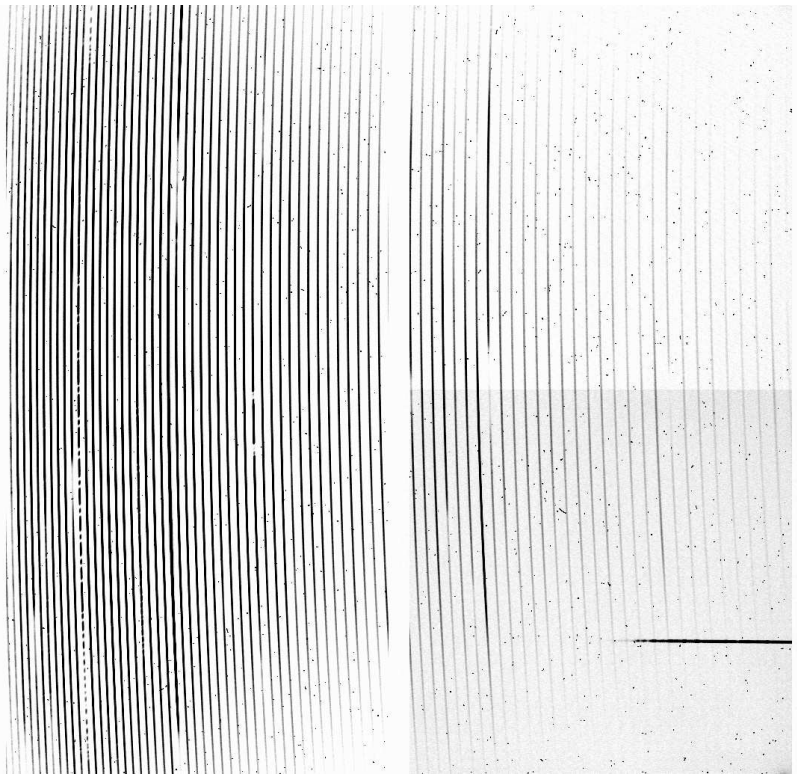

Table of Contents

1 Background

The reduced Chiron spectra available from the Yale software are in a 2-dimensional fits files which store the wavelength solution and the extracted data[1]. The reduction scheme is described by Tokovinin et al. (2013). The wavelength solution is obtained by running the IDL procedure *thid* (Valenti 1999), which performs a global 2-dimensional 6^{th} order fit (including cross-terms) to the echelle format data. The data are extracted using a boxcar extraction scheme. A cosmic-ray correction is applied.

The reduction scheme is optimized for the type of data for which the spectrograph was envisioned to be used: short exposures of bright stars, primarily for radial-velocity work. For this, the data

[1]These fits files have the prefix **achi**, and will be referred to herein as the **achi** spectra or **achi** data.

reductions appear to work well. The radial velocities are certainly very stable.

The extracted spectra (orders m=64-123)[2] are divided by a flattened flat spectra, preserving the gross echelle response. While orders m=126-138 (roughly 4100-4600Å) also fall on the detector, they are not extracted. Furthermore, over 225 points well off the blaze are trimmed from orders. Exclusion of lower S/N data and retention of the blaze function makes sense for high precision radial velocity data analyses, but I am interested in something completely different.

I have been using Chiron in a way that was probably never envisioned by its creators: synoptic observations of galactic novae. The challenges with the novae are many-fold. While bright at discovery (typically 10^{th} mag, but up to 3^{rd} mag), they fade: we follow them down to V$\sim$18 in some cases (at which point essentially all the flux is in emission lines). This is below the nominal sensitivity of the acquisition camera, and so presents some challenges for the telescope operator. Other challenges arise from the fact that we use 10-30 minute exposures, so there is significant background and numerous cosmic rays. Finally, nova spectra are dominated by broad emission lines, with FWZI up to 10,000 km/s. Background determination is non-trivial when the emission line is broader than the echelle order!

In examining the extracted spectra (the **achi*.fits** files) I noticed the presence of narrow "absorption features" (figure 1) near the tops of some of the emission lines in some of the novae. Originally I thought that this might be a new phenomenon attributable to our unprecedented high-resolution synoptic coverage, but some of the physics failed to make sense. My conclusion was that at least some of these "features" might be due to incorrectly subtracted cosmic rays[3], but further examination suggests a more insidious problem: in some cases the bright emission lines themselves were being treated as cosmic rays, and being removed[4].

At that point I decided it was time to look into re-extracting the spectra. The code described here, written in IDL, does just that. It allows the user to re-extract the data, using both boxcar and (optionally) Gaussian extraction techniques. It extracts all the spectral points along the order, and 75 orders, from m=64 through m=138 (74 orders starting at m=65 in the case of the slicer mode). This now-accessible spectral region is illustrated in figure 2. The broader wavelength coverage requires a new wavelength calibration. A two-step cosmic ray masking is employed, and inter-order background is subtracted.

The inputs for all the code described below are the **chi*.fits** raw data files.

[2]in general, when I refer to echelle orders in this document I refer to the index in the extracted two-dimensional array. This runs 0-n, where n is 73 or 74 for, respectively, slicer-mode or fiber-mode extracted data. Extracted order i corresponds to physical order m=$138 - i$. The Yale extractions in the **achi** files run from 0-58, or physical orders m=123 to 64.

[3]First suggested by U. Munari in the case of an apparent narrow reversal in Hα on one occasion in N Oph 2015.

[4]Sometimes being slow to publish has its benefits.

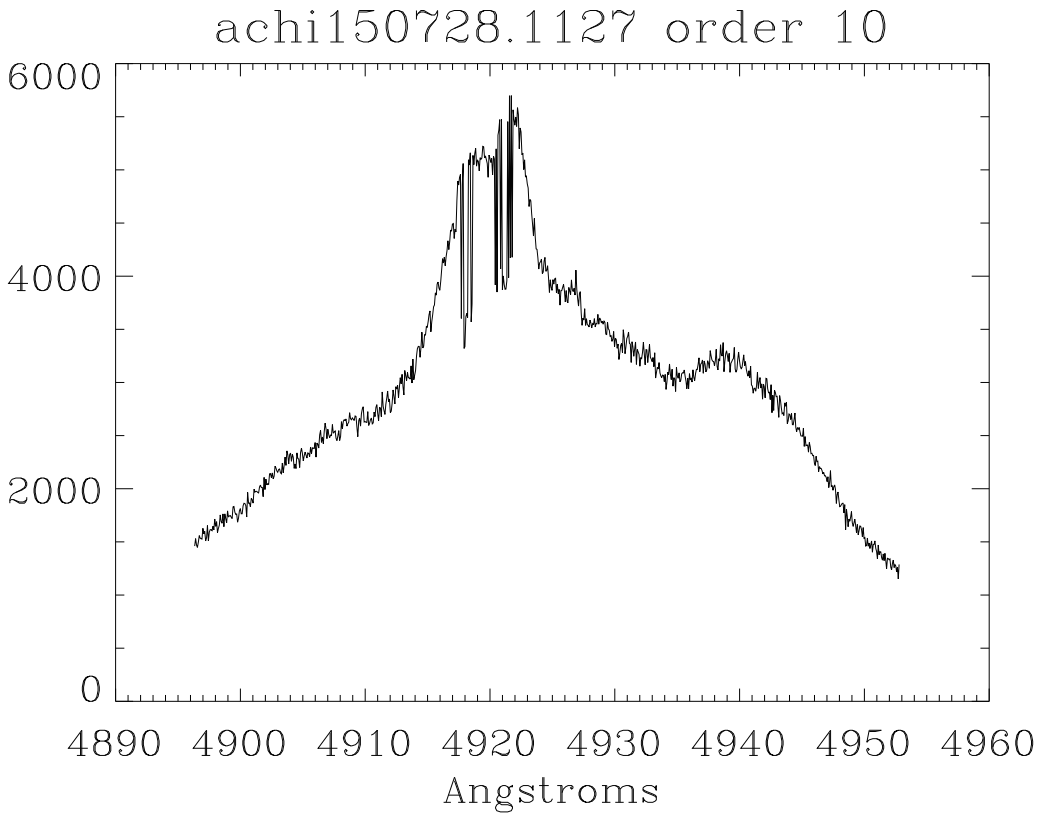

Figure 1: Order 10 of **achi150728.1127.fits**. The target is the nova N Sgr 2015b. The emission line is Fe II λ4921. The narrow dropouts are an artifact of the standard data reduction process.

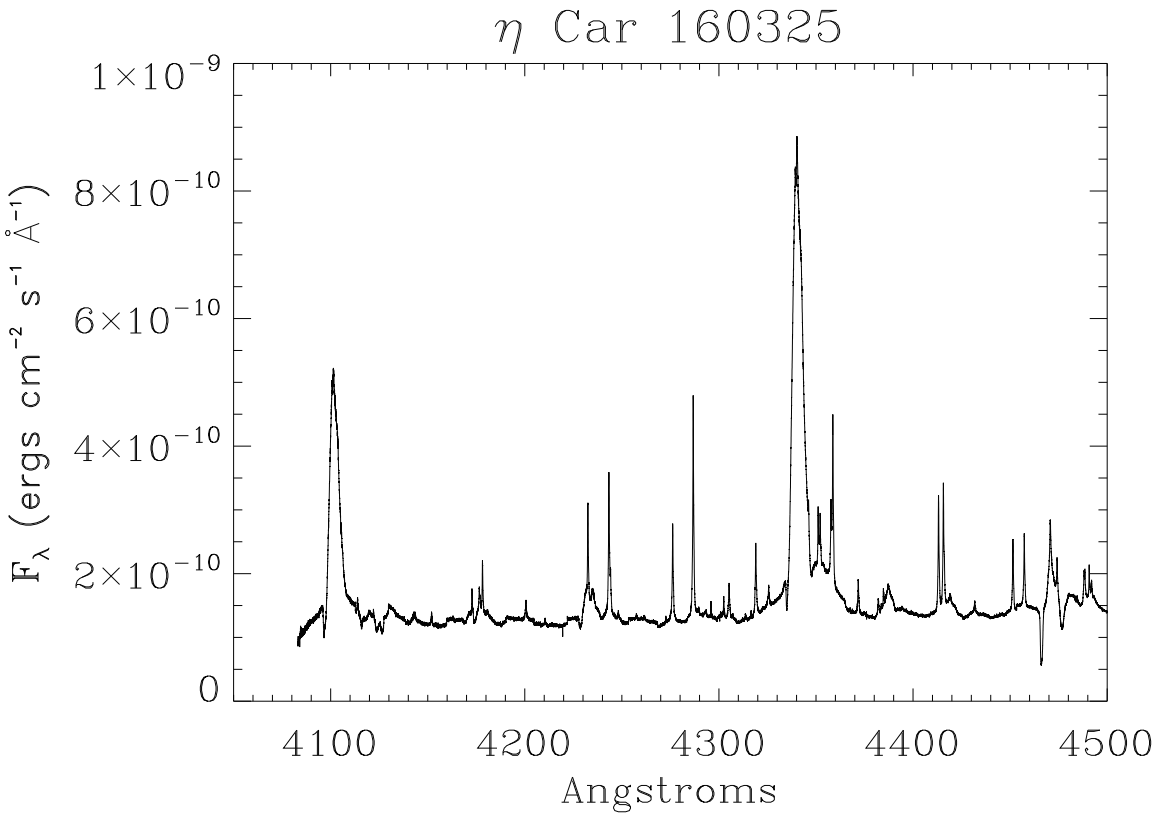

Figure 2: What you've been missing. Orders 124-138 in a slicer-mode spectrum of η Car. The extracted data have been flux-calibrated, and the orders have been spliced. The strong broad lines are Hδ λ4101Å and Hγ λ4340Å. Narrow blueshifted wind absorption is visible in both lines. The narrow emission lines are mostly Fe III.

Table 1: **Calibration File Names**

description	Fiber-mode	Slicer-mode	Format
flat field image	quartz.fits	slquartz.fits	* x *xlen*
trace extraction	trace_*yymmdd*.sav	sltrace_*yymmdd*.sav	*xlen* x N_{ord}
extracted flats	flats_*yymmdd*.sav	slflats_*yymmdd*.sav	*xlen* x N_{ord}
extracted ThAr spectrum	thar*yymmdd*.sav	slthar*yymmdd*.sav	*xlen* x N_{ord}
wavelength solution	*yymmdd*_cfits.sav	sl*yymmdd*_cfits.sav	see table 2

notes:
yymmdd is the civil date the data were obtained.
files are in the calibration directory yymmdd_cals.
xlen is 1028 for the fiber and 4112 for the slicer.
N_{ord} is the number of extracted orders.

2 Calibration Data

There are 3 essential components to the calibration process:

- order trace extraction,
- flat extraction, and
- wavelength calibration.

The calibration process is similar for the fiber and slicer. Output calibration file names (table 1) are prepended with **sl** for slicer-mode data.

In preparation for the first two items, I co-add all the flat images taken in the appropriate mode and save that image to disk. I trim the data and subtract the overscan, using the regions defined in the fits header, prior to co-adding the images.

2.1 Trace Extraction

I use the coadded flat image for tracing the orders. Orders are aligned roughly vertically in the images. I extract a subimage from y=500 to 550, where the middle of the chip is at y=513.5 (multiply by a factor of 4 for slicer mode)), and collapse this into a vector using the *median* function. I identify the N_{ord} highest peaks (N_{ord}=75 for the fiber and 74 for the slicer because of order crowding at the red end). I test for missing orders and discrepant peaks, and identify the central positions of the orders. I trace these orders by centroiding the sum of 21 points centered every 10^{th} point, and then fit this with a third order polynomial. The trace is stored in a *xlen* x N_{ord} array, which is written into an IDL save file (table 1) in the calibration data directory.

The trace extraction in fiber mode is clean because the orders are well-separated amd cleanly peaked. This is not the case for the slicer. The cross-order profile is broad and triple-peaked. I identify the center of the order as being half-way between the minima on either side. Crowding of the orders at the red end (low order numbers) complicates matters, to the extent that I chose to ignore order 64.

I also determine and save the width of the trace, for use in doing the boxcar extractions of the data.

Because of the stability of the instrument, it is not necessary to extract a new trace each night. I find that using a master trace file, shifted as necessary in the cross-dispersion direction, suffices.

2.2 Flat Extraction

Flats are extracted two ways: boxcar extraction and Gaussian extraction. These techniques are outlined below.

2.2.1 Boxcar Extraction

In this scheme, the data within $\pm wid$ pixels of the location of the trace at that Y position are summed. The width of the fiber-mode extraction slit is ± 3 pixels (set empirically). If fiber-mode, background is extracted on either side of the flat with a width set by the distance to the adjacent orders, less twice the extraction slit width. Following extraction, the two background spectra are filtered to remove discrepant narrow features, and averaged. This is not possible for the slicer-mode except at the bluest wavelengths because of order-crowding. Rather, a global background fit between the orders is subtracted prior to the data extraction.

Because I keep track of the counts in the extracted spectrum and the background regions, I keep track of the $\sqrt{N}$ statistics and propagate the errors. The errors are stored as a S/N vector because this is invariant when the fluxes are scaled.

2.2.2 Gaussian Extraction

In principle, extraction using the PSF can be optimal because cosmic rays and other defects will deviate from the "known" profile. In practice, here I fit cuts across the spectrum with a Gaussian profile, which is probably not the appropriate functional form. Because the closeness of the orders can make it hard to constrain the background, I simultaneously fit three adjacent orders, except for the first and last orders. where I only fit two. There are 12 free parameters (3 in the background and three in each Gaussian). The fits to the outlying orders are discarded. The background is extrapolated under the central Gaussian. The relevant parameter is the analytic integral of the Gaussian (which is presumably less affected by outlying points than is a straight summation of the data).

The fitting is done using the *mpfitfun* (Markwardt) function with constrained fits. The initial fit is made to the sum of the 5 pixels at the center of the image (Y=514). Subsequent fits going

outward towards the top and bottom of the image use the previous fit as initial estimates. The position of the Gaussian is constrained to deviate from the previous fit by less than 1 pixel, and the width is constrained to deviate by less than 20%. Note that because the initial estimates depend on the previous fit, the solution can run away and settle on another order. This is not a problem for the flats or for bright sources, but can be for faint objects. Therefore I have an optional iterative fitting process, where the position and width of the initial extraction are forced to those of the trace extraction. In the second iteration these constraints are relaxed (see §3.2), with the position free to move by ± 0.5 pix, and the width free to vary by $\pm 10\%$ from the values from the fit to the trace. This reduces the likelihood that the solution will run away.

Gaussian extraction is probably not possible for slicer-mode data.

2.2.3 Comparison of Extractions

The boxcar- and Gaussian-extracted flats agree with each other (to within a normalization factor) to better than 1%, although there is significant structure (see figure 3). The structure correlates with the width of the Gaussian fit across the order.

The boxcar extraction is flatter, relative to a low order polynomial, by a factor of 2, than is the Gaussian extraction, so at first look it seems that the boxcar extraction is to be preferred. However, because of the stability of the instrument, the structure in the Gaussian flat largely cancels out (figure 4), and the two extractions are comparable, even for reasonably high S/N spectra. In principle the Gaussian extraction provides better cosmic-ray rejection, but it also takes significantly longer to run (see §5.8).

Division by the flat, rather than by the flattened flat, yields a reasonably flat extracted order (Figure 5) which simplifies flux-calibration and order-splicing. Short of that, measurements of spectral features are often easier on flat continua.

2.3 Wavelength Calibration

I was unable to get good wavelength solutions using the *thid* code. Eventually I decided to do a wavelength solution the old-fashioned way. I selected one order and, using the *thid* solution as a starting point (see §5.2), obtained a wavelength solution. One can also use the wavelength solution in the appropriate **achi** file for a starting point. Then it becomes a matter of identifying the correct wavelengths and fitting the data positions of the lines. I fit these with a polynomial. Using the properties of the echelle, that $m\lambda$ is constant as a function of the Y coordinate between the orders, I made an initial wavelength solution for each order, and then edited each order, removing blends and weak lines. The air wavelengths of the lines come from **thid_data.xdr**.

My master solution, derived for the fiber on the night of 150728, contains some 1300 lines in 75 orders. The RMS scatter in the solutions for each order are good to better than 1 km/s.

This solution can then be migrated to other dates, doing a cross correlation of the "good" line list with the extracted Th-Ar spectrum to generate a gross shift, and then automatically re-fitting

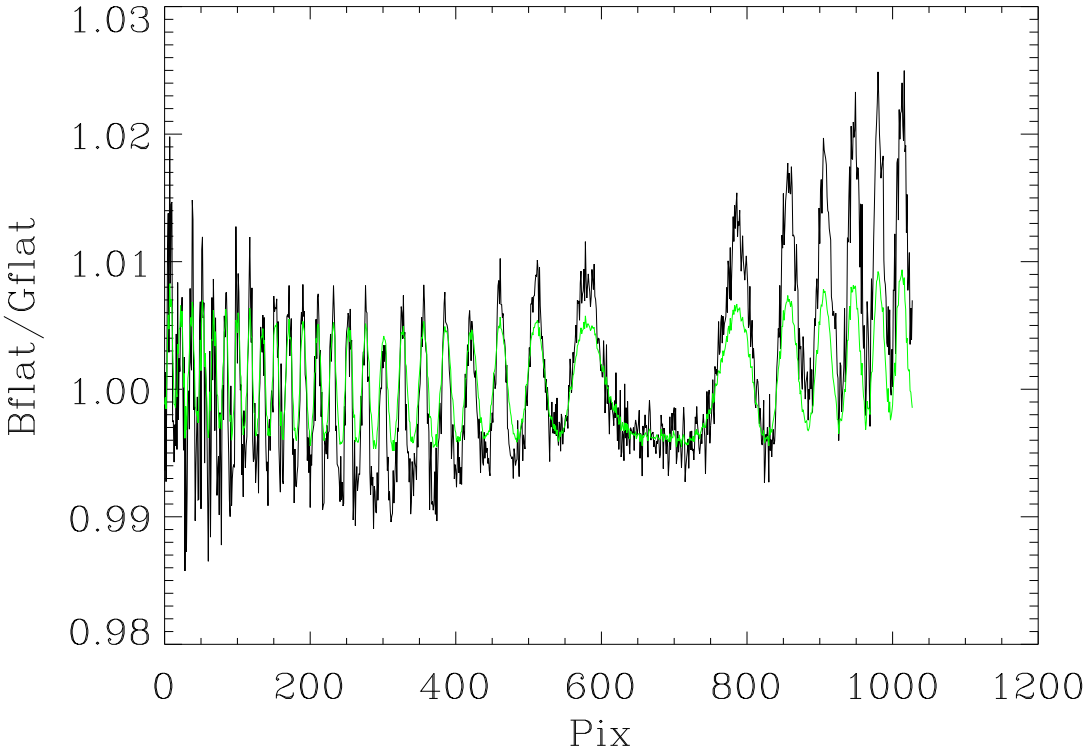

Figure 3: The normalized ratio of the boxcar-extracted to the Gaussian-extracted flat for order 108. The green trace is the scaled width of the Gaussian used to extract the flat. They track well, with the larger ratio (less flux in the Gaussian extraction) when the fit is broader. This occurs when the trace is centered between two pixels. I suspect this is attributable to the non-Gaussianity of the PSF. In any event, the effect seems to divide out (see figure 4).

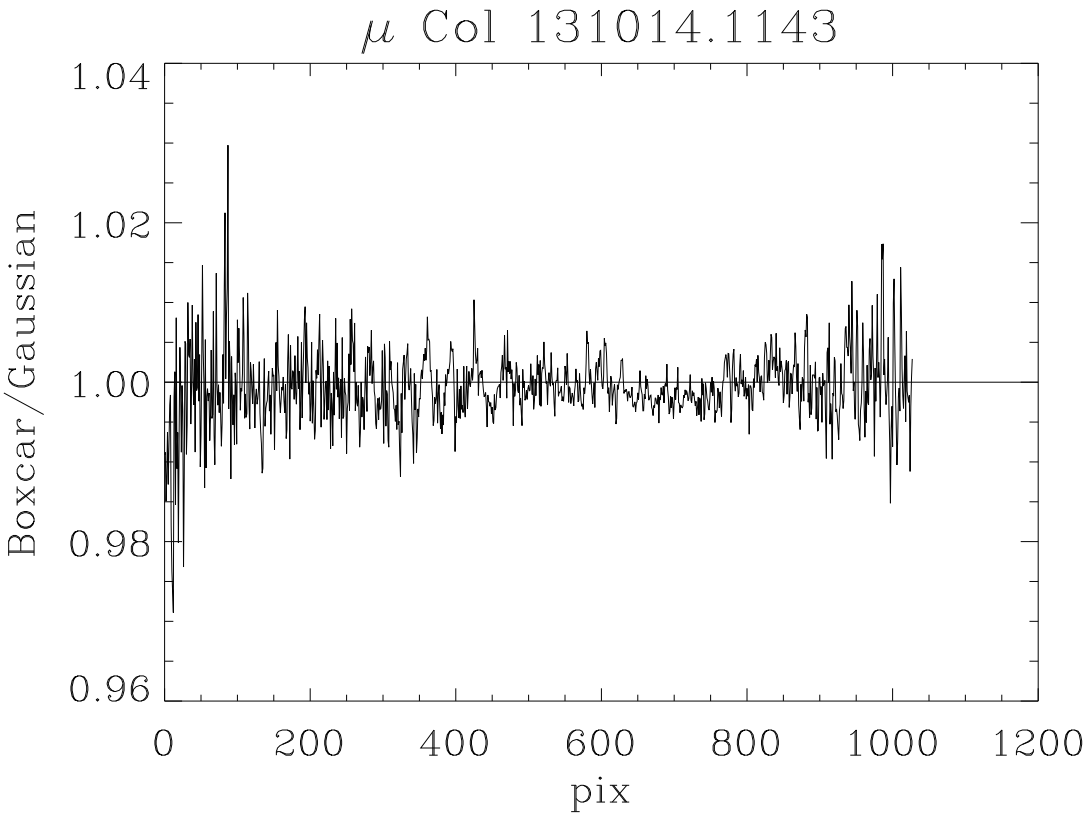

Figure 4: The ratio of the boxcar-extracted to the Gaussian-extracted spectra, after flat division, for order 108 of chi131014.1143 (μ Col). The RMS scatter of the ratio is 0.6%. The median is 0.999; no normalization has been applied. The structure visible in the flat ratio (figure 3) is greatly reduced. The SNR of the spectrum, from counting statistics alone, peaks about 900, and exceeds 500 between pixels 250 and 850. Within this region the RMS is about 0.4%, comparable to the 0.3% expected from counting statistics alone.

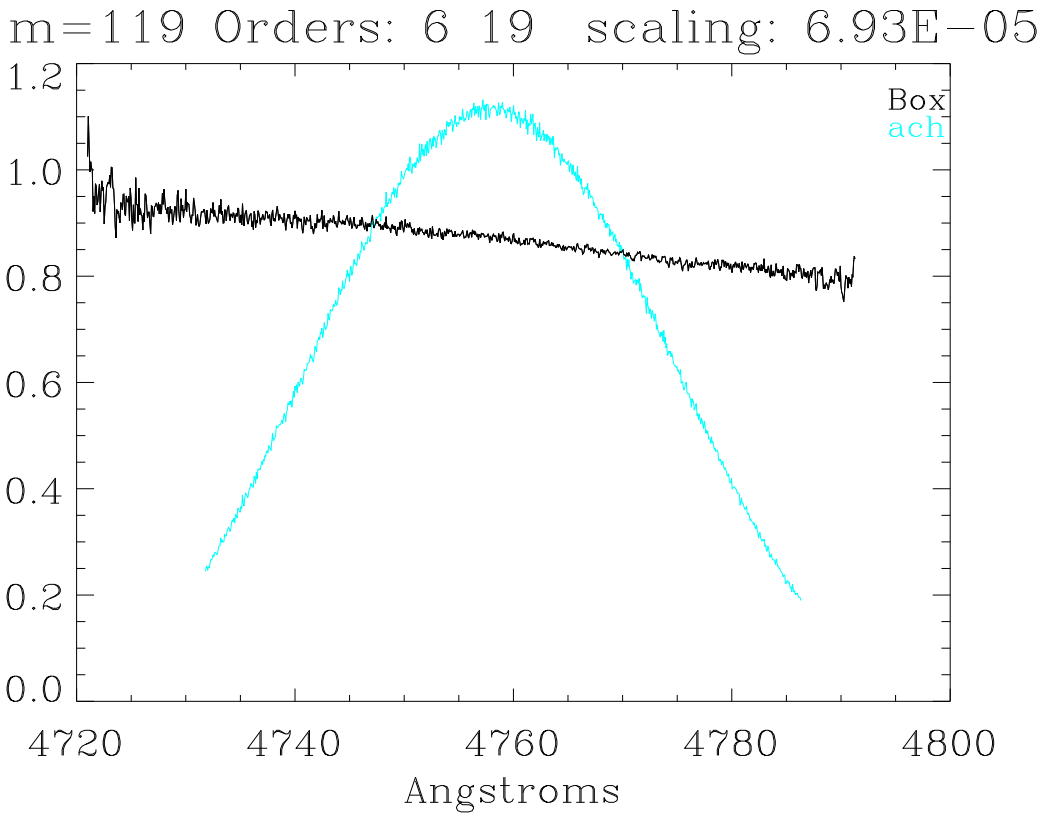

Figure 5: A particularly boring part of the spectrum of the O9.5V star μ Col, a spectrophotometric standard. Note that division by the actual flat extraction yields a very flat spectrum.

Table 2: **ths Structure Tags**

Tag	Format	Description
cfits	dblarr(9)	coefficients of polynomial fit (up to 8^{th} order)
sdv	float	standard deviation of polynomial fit: units=pix
np	integer	Number of lines fit
m	integer	physical order number (138 - 64)
pixfit	fltarr(np)	X pixel of fit position
wavfit	fltarr(np)	air wavelength of fit position
diff	fltarr(np)	wavelength - fit wavelength
wid	fltarr(np)	Gaussian FWHM of line
mlam	dblarr(3)	mλ for pixels 0, 514, and 1027
xcut	intarr(2)	currently unused
mres	double	mean resolution E/δE

the individual lines. The goodness of the solution is estimated by plotting mλ as a function of X-position for all the lines fit. There is an irreducible order-dependent scatter of up to $\pm$ 60Å in mλ after subtracting the best fit third-order polynomial. The 150728 solution maps well into all the Th-Ar spectra obtained (starting with 120324) - a strong testament to the stability of the instrument.

Verification of the wavelength solution is based on looking for significant deviations in mλ from that expected, and consequently in the length of the order in wavelength space. Deviant lengths are generally due to poorly-constrained solutions near the ends of orders with few lines near the order extrema. Refitting with a lower order polynomial usually fixes the problem.

The wavelength solution is written to an IDL save file (table 1). The file contains a structure, *ths* which has one element per order fit. The tags are listed in Table 2. Note that the *pixfit, wavfit, diff*, and *wid* tags are padded to 60 element arrays.

It is important to realize that, while I need a reliable wavelength solution, I do not need one with the fidelity of the Yale solution. Consequently, I have neither examined nor tweaked the solutions on most nights for the best possible solutions. But they look pretty good (see figure 6).

For slicer mode I start with the fiber solution, and search for lines at the predicted pixel location for a quadrupled resolution. It seems to work - see figure 7.

2.4 Flux Calibration

Conversion from counts to flux requires observation of a flux-standard star under photometric conditions. Since many factors come into play (e.g., seeing, slit width, wavelength-dependent slit losses, etc.), I use the flux-standard to establish the shape of the instrumental response. Absolute

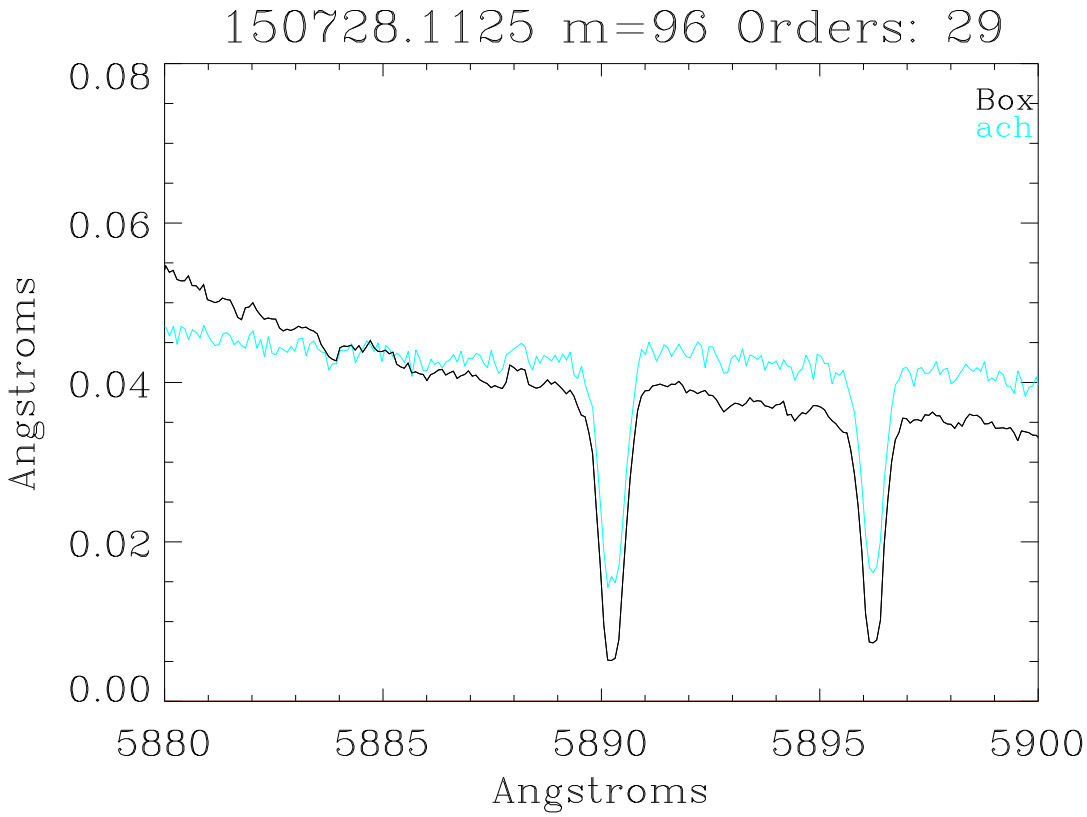

Figure 6: The Na D lines in N Oph 2015 on 150728. There are few narrow lines in novae - these are interstellar. The **achi** spectrum is in aqua. The wavelength solutions are in good agreement.

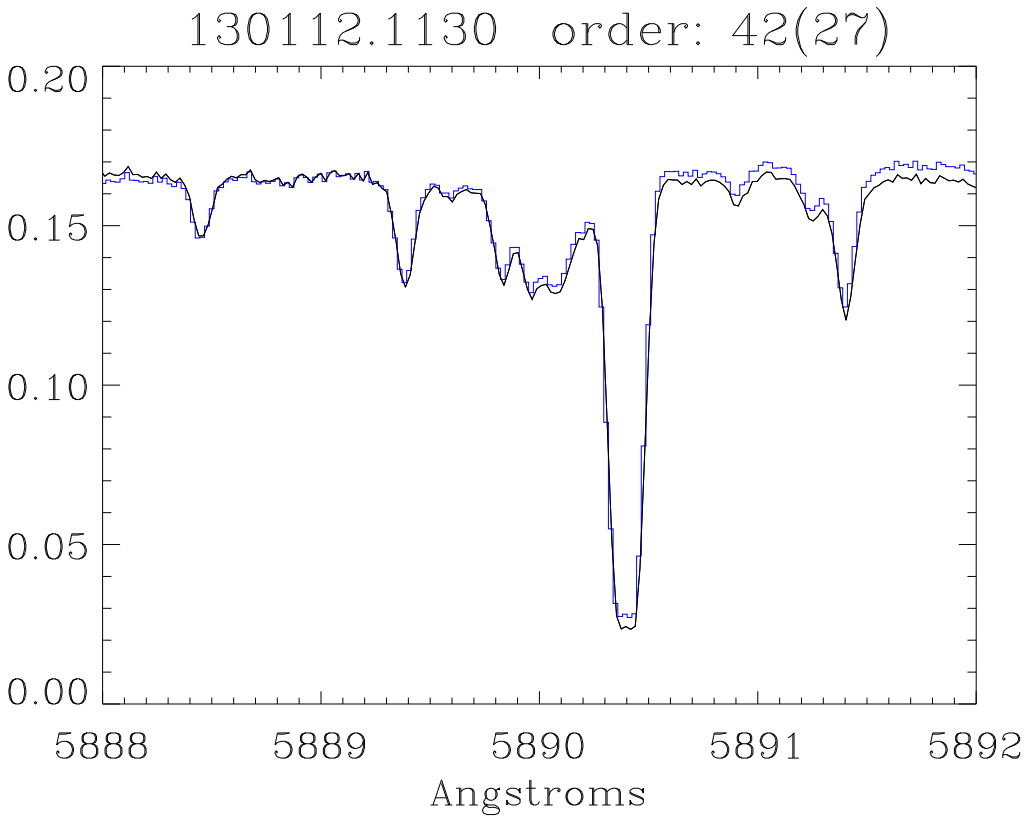

Figure 7: A comparison of the slicer mode spectrum of σ Ori using my reductions (black) and the spectrum from the **achi** file (blue) processed using the Yale reduction. This is a portion of order 42 (order 27 in the achi file) containing the Na D_1 line. The difference in slope is attributable to fact that I divide by the extracted flat, while the achi spectrum is not flattened. A heliocentric correction is applied to both spectra; fluxes are normalized to the median in the plotted region. The spectra match well; there is a wavelength offset corresponding to 0.4 km/s between the spectra that could arise from many sources.

calibration (at least for a variable star) requires simultaneous photometry. I have used μ Col (HR 1996), a bright star

3 Data Reduction

3.1 Cosmic Rays

In most cases, I have taken single exposures in order to maximize S/N in a given time. This comes at the expense of contamination by cosmic rays. The propensity of the default reductions to flag and remove strong emission lines is a major motivation for this reduction effort.

There are two cases to consider: cosmic rays on or near the order, and those in the background.

Cosmic rays in the background are the less serious issue. Filtering, and then averaging, the background spectra on either side of the order efficiently removes most small-scale blemishes. In the Gaussian extractions I fit 4 interorder regions, ensuring that small features will have a minimal effect.

However, most cosmic ray detection algorithms look for sharp edges, very much like the dispersed spectrum, and this can cause difficulties. I originally tried a direct application of the *la_cosmic* procedure (van Dokkum 2001), and found that it tended to chew up the spectra. After some experimentation, I decided to pre-filter the data with a 1x5 median filter. This has the beneficial effect of removing sharp features in the dispersion direction, while only minimally reducing resolution for sharp features. Then an application of *la_cosmic* seems to do a better job, but it still has trouble with the bright Hα emission line in many novae (and also with other narrow emission lines). So I incorporated a keyword to let one ignore any masked data in the immediate vicinity of Hα.

Alternatively, the *dcr* (Pych 2004) algorithm can be used too, by specifying the *dcr* keyword in the call to *ch_reduce*. The user will need to install the *dcr* executable. A customized **dcr.par** file is written in the working directory. The *THRESH, XRAD, YRAD, NPASS*, and *GRAD* values can be set via keywords. I've modified the default values for *XRAD* and *YRAD* to 4 and 31, respectively. When *dcr* works, it gives about the same results as does *la_cosmic* as implemented here, though it seems to miss more cosmic rays, especially in high S/N spectra. It may be possible to fine tune the parameters to do a better job. *dcr* runs much faster than *la_cosmic*. However, it seems to be unstable, in that varying the *XRAD* and *YRAD* can give wildly divergent results, including clearly unphysical continuua. *dcr* seems to remove low points as well as high points, which can get it into trouble near the ends of orders.

The data quality vector (see Tables 3 and 6) encodes pixels affected by cosmic rays, as well as saturated pixels.

If you have a spectrum with lots of narrow emission lines (as in a nebulosity), running *ch_reduce* with the *noclean* keyword set prevents the code from interpreting narrow emission lines in the spectrum as cosmic rays. I have specific exceptions built in to prevent the code from interpreting narrow telluric Na D and O I λ6300 emission as cosmic rays.

Table 3: **xchi*.fits file contents**

Index	Description
0	Wavelength solution
1	Boxcar-extracted data
2	Signal-to-noise ratio
3	data quality
–	Gaussian-extracted data
–	Flux-calibrated data (see §5.4)

I found that the *la_cosmic* algorithm tends to flag enormous numbers of bad pixels in the slicer-mode images, perhaps because they tend to be noisier than fiber-mode data, or because they occupy more of the useable area on the chip. By default there is no cosmic ray rejection performed for slicer-mode images. However, the spectra are cleaned in the post-processing (§5.4).

A caution: use cosmic ray rejection cautiously. If something looks peculiar, rerun the extraction with the /nocr flag set. See figure 8. The best way to filter cosmic rays is to take 3 images and median-filter them.

3.2 Data Extraction

The basic extraction techniques are described in §2.2.

The trace is cross-correlated (in X) against the image in order to find any bodily shift between the spectrum and the flat.

Boxcar extraction uses the same slit width employed for the flat extraction.

Gaussian extraction can be specified, either with 1 or 2 passes, as described in §2.2.2.

The data are flattened by division by the appropriate flat extraction. Because the blaze function is not removed beforehand, the continua are more-or-less flat.

The extracted data are written out into an **xchi*.fits** file, with a format similar to the **achi*.fits** file from the standard extractions, except that the data are an Nx*xlen*xN_{ord} array, rather than a 2x801x62 array. The first two images (N=0,1) are the wavelength solution and the boxcar-extracted spectra, as in the **achi*.fits** files. The other indices are described in Table 3. An absent index means that the image is assigned dynamically, with the index recorded in the fits header.

More data, defined in Table 4 are saved in the **xchi*.sav** file. In Table 4 *nord* refers to the number of extracted spectra, N_{ord}.

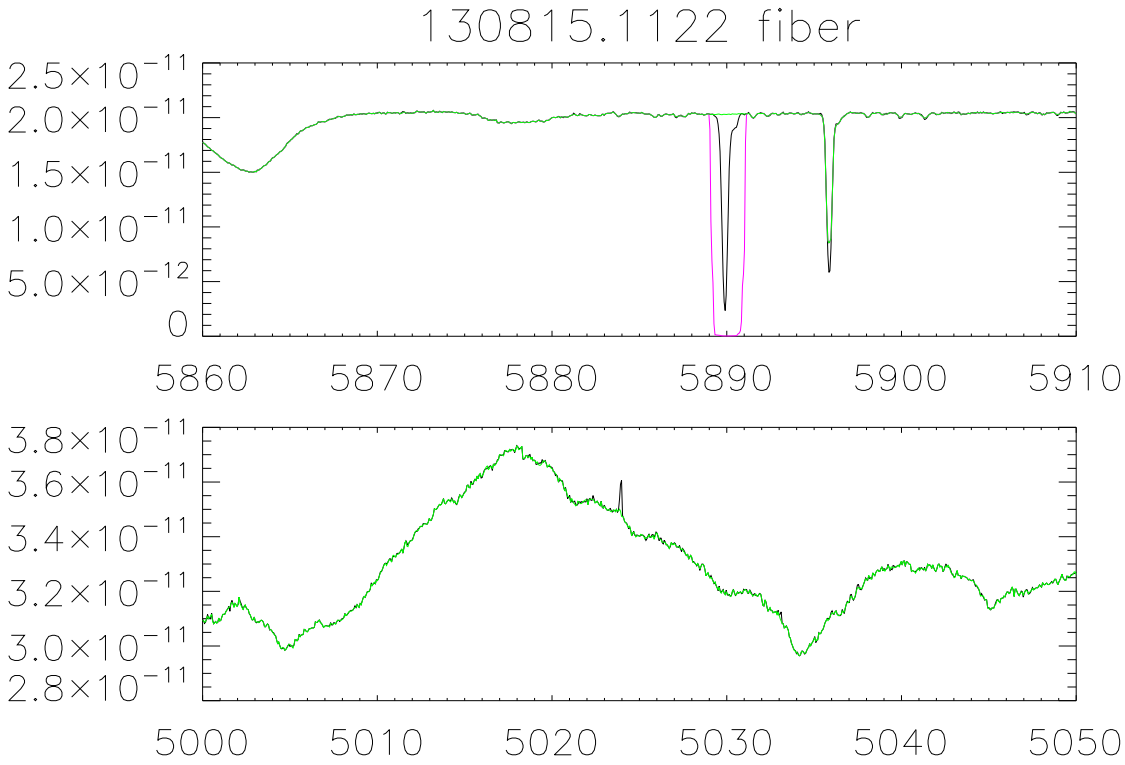

Figure 8: These panels illustrate the effects, both good and bad, of cosmic ray filtering single images. The lower panel shows how cosmic ray rejection is supposed to work. The black trace is the boxcar-extracted spectrum with cosmic ray detection turned off (/nocr); the green trace is the same extraction with nominal CR rejection using the *la_cosmic* software. A narrow positive deviation, seen in black, is rejected (this results from setting *spfitord=0*; the default setting of *spfitord=2* finds and rejects this event). The upper panel shows what happens when a real narrow feature is mis-identified. The default extraction produced the green trace. Note the absence of the strong interstellar Na D_1 line. The magenta trace is the extraction run with CR rejection and with the */noclean* keyword set. Points flagged as bad by *la_cosmic* are set to zero. If the */noclean* keyword is not set the flagged points are interpolated over (the green trace). Setting the */nocr* keyword results in the black spectrum, and a normal-looking pair of Na D lines. This is a fiber-mode spectrum of V339 Del shortly after maximum.

Table 4: **xchi*.sav file contents**

Variable	format	description
FILELOG	structure	header information
H	strarr(*)	FITS header
MASK	bytarr(*, *xlen*)	mask image from *la_cosmic*
THS	structure(nord)	defined in Table 2
XFITS	fltarr(*xlen*,nord)	traces
	Boxcar Extraction Parameters	
BACK	fltarr(*xlen*, nord)	background spectra
BDATA	fltarr(*xlen*, nord)	net extracted spectrum
BDQ	intarr(*xlen*, nord)	data quality flags
BDX	fltarr(*xlen*, nord)	extracted, flat-fielded spectra
SNR	fltarr(*xlen*, nord)	SNR for BDATA, BDX
WID	fltarr(*xlen*, nord)	extraction width = 2*wid+1
	Gaussian Extraction Parameters	
GDATA	fltarr(*xlen*, nord)	net extracted spectrum
GDQ	intarr(*xlen*, nord)	data quality flags
GDX	fltarr(*xlen*, nord)	extracted, flat-fielded spectra
	Other	
FN	fltarr(*xlen*, nord)	fluxed extracted spectrum
DS	fltarr(*xlen*, nord)	data removed in spectral cleaning

4 Data Organization

All data and calibration data are stored in the directory *chirondata*. The cshell definition is

```
setenv chirondata YourDataDirectory
```

Create a subdirectory *cal* under *chirondata*.

Tar files downloaded from the Yale archive should be saved and unpacked in the *chirondata* directory. Each night will be in a subdirectory named YYMMDD, the observation date.

Calibration data should be downloaded to and unpacked in *chirondata/cal*. There will be a series of directories of the form YYMMDD_cals.

Extracted and derived calibration data are saved in the *chirondata/cal* subdirectories. Extracted spectra are saved in the *chirondata* subdirectories.

All procedure file names are lower case; on occasion in this document I have spelled them with mixed cases to improve readability.

5 The Cookbook

The code is written in IDL, and was tested under version 8.1. The process of calibrating and reducing a night's data is easily divided into three parts[5].

5.1 Basic Calibrations

The data must be in the *chirondata/cal/YYMMDD_cals* directory (see §4). *Ch_Cals* reads the calibration data, and

- co-adds the flat images,
- traces the orders in the flat images,
- extracts and writes the flat orders,
- extracts and writes the Th-Ar spectrum, and
- computes the wavelength solution.

The files written in the process are listed in table 1.

```
Ch_Cals: reduce Chiron calibration images
* calling sequence: Ch_Cals,day
*    DAY: 6 digit string (yymmdd); required
```

[5] *Omnes data in tres partes divisa est.*

```
*
* KEYWORDS:
*    DOGAUSS:   set to enable Gaussian extraction of flat
*    EXAMINE:   set to examine each extracted order (sets plt)
*    FIXWID:    sets fixed extraction width
*    FORCE:     set to remake the quartz.fits file
*    MKTRACE:   set to make new trace (2 to lookup w/o shifting)
*    MODE:      default=fiber
*    NOWAVCAL:  if set, skip wavelength solution migration
*    PLT:       set to follow the extractions by plotting the extracted orders
*    REFTHAR:   index of reference ThAr spectrum, def=first
*    SLICER:    shorthand for mode='slicer'
*    USEFLAT:   set to use pre=extracted flat for this day
*    WCALONLY:  set to redo ch_migratewcals
```

You must run *Ch_Cals* independently for each observing mode you wish to calibrate. Set the *dogauss* keyword only if you intend to do Gaussian extractions in fiber mode. Gaussian extraction is slow because it requires fitting a Gaussian profile at each point in each order. Gaussian extraction is not enabled for slicer data.

Unless the keyword *nowavcal* is set, the default wavelength solution will be migrated to this day, using the Th-Ar spectrum for this day. See §5.2 for more details.

If multiple Th-Ar observations exist, all images are cross correlated against the reference ThAr image (by default, this is the first of the ThAr images; change this with the *refthar* keyword)). The resulting pixel shifts are saved in the extracted ThAr .sav file. The instrument is stable: the drifts over the night of 21 July 2017 (fiber mode) are shown in Figure 9.

Set the *plt* keyword to see the extracted flat orders. Set the *examine* keyword to pause after each order is plotted. While paused, type "z" to get an IDL prompt; type any other key to continue.

The wrapper *Do_ChCals* runs *Ch_Cals* on multiple directories. You can use *Ch_CalStatus* to list directories that have yet to be calibrated.

5.2 Wavelength Calibration

For many of these routines, you will need the Th-Ar line list in **thid_data.xdr**. This file should be saved as **chirondata/cal/thid_data.xdr**. You will also need the extracted ThAr save file file generated by *ch_cals*. The wavelength solutions are stored in
chirondata/cal/YYMMDD_cals/xYYMMDD_cfits.sav, where **x** is **sl** for slicer spectra and null for fiber spectra.

These routines use a number of common subroutines. In *plwfit*, commands are entered by single keystrokes as defined in Table 5.

The basic routines used in wavelength calibration are:

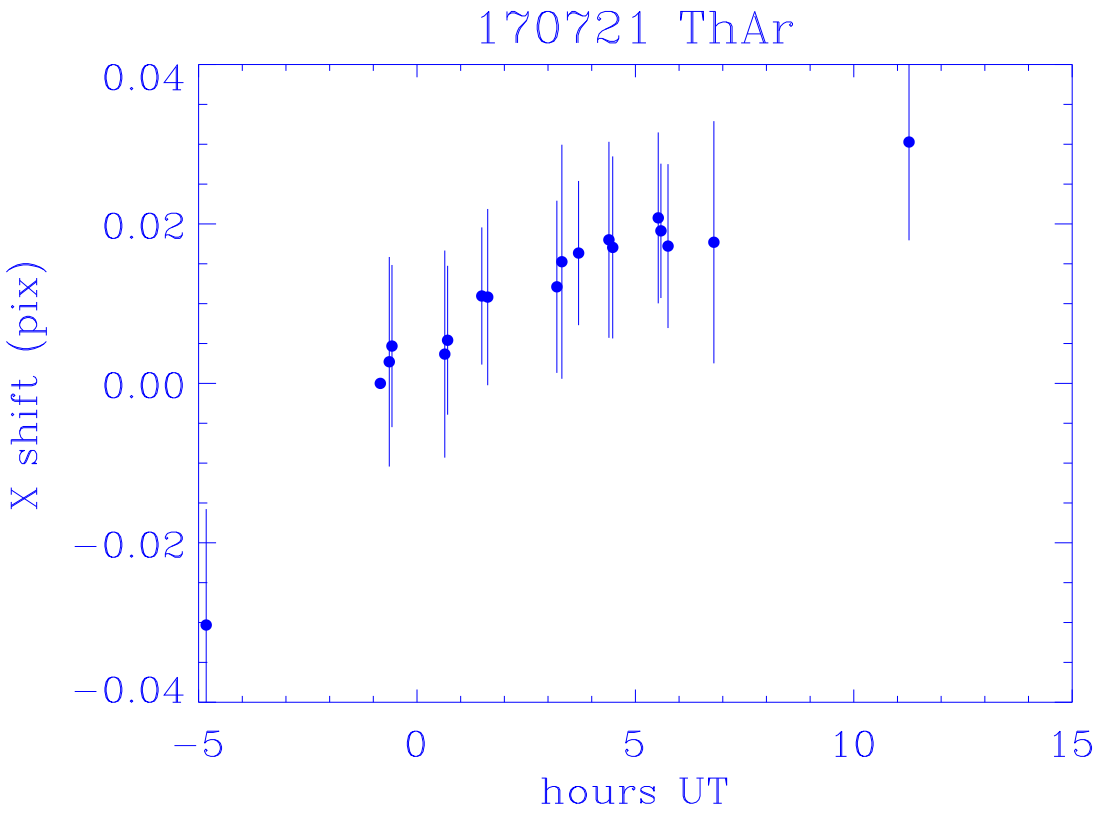

Figure 9: The drift in pixels over the course of a night of the Th-Ar spectra in fiber mode. The drift correlates well with various instrumental temperatures. While the drift is systematic, and is accounted for in the extraction software, it is also insignificant for many purposes. *Chiron* is stable.

Table 5: **WCal Keystroke Commands**

Key	Description	Notes
e,E	examine fit to line	2
m,M	mark line (2 keystrokes)	1
q,Q	exit	1,2
r	refit data	1,2,3
R	refit data after changing polynomial order	2,3
s,S	restore all deleted points	2
x,X	delete point closest to cursor	1,2
z,Z	stop	1
>	jump ahead	1
<	jump back	1
space	mark line center	

Notes: 1: used in *ch_setwcals*
2: used in *plwfit*
3: case-sensitive

ch_setwcal: Initial setup. This runs *thid* on the Th-Ar lamp image to determine the initial wavelength solution. *thid* does not converge as well as I think it should (or as it used to, for the BME), but typically 300-500 lines are fit. The user specifies the order to fit (using the *startord* keyword, and the order of the polynomial fit (*ford*; default=5). The number of Th-Ar lines plotted is set by the *minflux* keyword. By default, all lines stronger than 0.8 of the mean intensity are plotted. Decrease this value to see more lines. Note that the tabulated line intensities do not necessarily correlate with the observed intensities. The Ar lines are also used. No checking is done for saturated lines.

Two plots are generated. One shows the difference in pixels between the observed and predicted line location as a function of wavelength. The other (the active window) shows a portion of the spectrum with lines from the this list marked. Vertical magenta lines have been fit; dotted yellow line have not. Use the > and < keystrokes to navigate. Going beyond the long wavelength end of the spectrum or typing *Q* exits this part of the program. Use the *M* key to add lines to the fit. First mark the yellow dotted line, then mark where it should be in the data. The Y level of the cursor sets the baseline for the Gaussian fit. The fit line center will be shown in green. Mark a line for exclusion with the *X* key.

Use the > key to get past the end of the spectrum to move on. Then the data will be fit using *plwfit*. Useful keystrokes (see table 2) include *e,x, and r*. Only the *r* command is case-sensitive.

ch_tweakwcals: use to tweak an existing wavelength solution for one order. Call it as **ch_tweakwcals,YYMMDD,order=x,mode=mode**.

ch_migratewcals: use to migrate a wavelength solution from one day to another.

```
* Ch_MigrateWcals - migrate one Chiron wavelength solution to a different day
* calling sequence: Ch_MigrateWcals,date
*    DATE: date in format YYMMDD, no default
*          Ch_Cals must have been run for this date
*
* KEYWORDS:
*    AUTOFIT: def=2; 1 to examine each fit
*    EXCLSIG: automatic line exclusion, def=2.5 sigma from initial fit
*    MINFLUX: def=0.8 of mean of Th-Ar intensities
*    MODE:    default='fiber'
*    ORDERS:  set for select orders
*    REFFIT:  reference fit date (YYMMDD), def="chiron_master_wcal"
*    THRESH:  threshold counts in line for autofit, def=20
```

ch_examinewcals: non-interactive examination of the solution. It plots the deviations of the fit mλ after subtracting a third order polynomial. Outliers are flagged, and orders that are too long or too short are identified so they can be refit. Do this by running **ch_examinewcals,/redord**, which uses **ch_tweakwcals,/redord** on the flagged orders.

ch_extendwcals: use to apply the solution for one order to another order on the same night.

ch_wcalsummary: generates a summary of each wavelength solution (one line per order). The last column, the mean resolution, gives a good data quality indicator. It should be about 28,000 for fiber-mode data, and 78,000 for slicer-mode data.

Once you have a master wavelength calibration, you should be able to use **ch_migratewcals** and **ch_examinewcals** to calibrate all other days.

5.3 Data Extraction

The calibration files including a wavelength solution, must exist before data can be reduced[6]. The data must be in the *chirondata/YYMMDD* directory (see §4). To reduce a full night's data, merely run *ch_reduce,YYMMDD*. To reduce a particular spectrum, type *ch_reduce,YYMMDD,file=xxxx*, where xxxx is the 4 digit file number (**chiYYMMDD.xxxx.fits**). The file number **xxxx** can be either a string or an integer.

[6]You can calibrate the data using cal data from another night by specifying the date in the *caldate* keyword.

```
Ch_Reduce: reduce raw Chiron Spectra
* calling sequence: Ch_Reduce,date
*    DATE: 6 digit string (yymmdd); required
*
* KEYWORDS:
*    CALDATE:   set to date of calibrations, if not date
*    Do2:       set to coadd and extract a pair of images
*    Do3:       set to coadd and extract a triad of images
*    DOGAUSS:   1 or 2 for Gaussian extractions
*    EXAMINE:   set to examine each extracted order (sets plt)
*    FILE:      name of file; def = all
*    MODE:      default=fiber
*    NOCLEAN:   set to skip extrapolation over bad points
*    NOCR:      set to skip CR filtering
*    NOHAMASK:  set if H-alpha is in emission
*    NOPROC:    set to skip post processing
*    NOSAVE:    set to run code but to not save the data; stops when done
*    NSIG:      sigma cut for replacing bad points in Gauss fit. Not yet implemented.
*    OPTIMUM:   set for optimum extraction. Not yet implemented.
*    PREFILTER: 1xn filter, def=5
*    SPFITORD:  background order for ch_cleansp; def=2
*    STARTORD:  starting extraction order, def=0
*    UPDATE:    set to update single order
```

ch_reduce options:

- If the keyword *file* is not specified, all files in the specified mode will be extracted independently, If *file* is specified (as either a string or integer), only that file is reduced.
- The boxcar extraction is the default.
- A Gaussian extraction is specified (in addition to the boxcar) by setting the *dogauss* keyword to 1 or 2, for either single pass unconstrained fit or a constrained double pass fit (§2.2.2). Note that this option significantly slows down the execution time.
- If there is a strong Hα emission line, the cosmic ray filtering may wipe it out. See figure 11 for an example. This will happen in *ch_reduce* unless the *nohamask* keyword is set. This prevents the code from identifying the top of the Hα line as a defect, unless saturated.
- The clean algorithm identifies the pixels flagged as bad and interpolates over them. Use the *noclean* keyword to turn this off. All bad pixels are identified in the *bdq* vector (see Table 6).

Table 6: **Data Quality Flag**

Flag	Description
1	pixel flagged by *la_cosmic* in lower background slit
2	pixel flagged by *la_cosmic* in upper background slit
4	extracted data interpolated over single flagged pixel along spectrum
8	extracted data interpolated over single flagged pixel across spectrum
16	pixel flagged by *la_cosmic* in extraction slit
32	gaussian flat = 0
64	flagged in ch_cleansp
512	saturated pixel

- set *nocr* to see what happens in the absence of cosmic ray filtering. *nocr* is the default for slicer mode.
- Use the *update* keyword to reprocess a single order. Set update to the order number (0-74).

The output from *Ch_Reduce* is the files **xchiYYMMDD.xxxx.fits** and **xchiYYMMDD.xxxx.sav**, as described in §3.2.

5.4 Post Processing

Ch_reduce writes out the extracted, flat-fielded counts spectrum. Post-processing consists of a.) spectral cleaning b.) flux-calibration, and c). creating a spliced one-dimensional spectrum.

Spectral Cleaning: A final round of spectral cleaning is performed here. Points that exceed a set number of standard deviations above a local background are flagged as as outliers. The local background is a polynomial fit to a region100 points wide. The order of the polynomial is set by the keyword *spfitord*. The threshold is 5σ for orders up to 60, 6σ for orders 60-67, and 7σ for the reddest orders. Flagged points are interpolated. Turn this off with the *nospclean* keyword.

The lower panel of figure 8 shows that the spectral cleaning algorithm may not filter out small events (cosmic rays or hot pixels) above a variable background when *spfitord* is 0 or 1. Re-read section §3.1

Flux Calibration: I calibrate the response using a fiber-mode spectrum of μ Col obtained on 131014, or a slicer-mode spectrum of μ Col obtained on 131008. In each order the counts are ratioed to the modeled spectrum[7]. The modeled spectrum is low resolution: I smooth over

[7]available at https://www.eso.org/sci/observing/tools/standards/spectra/hr1996.html

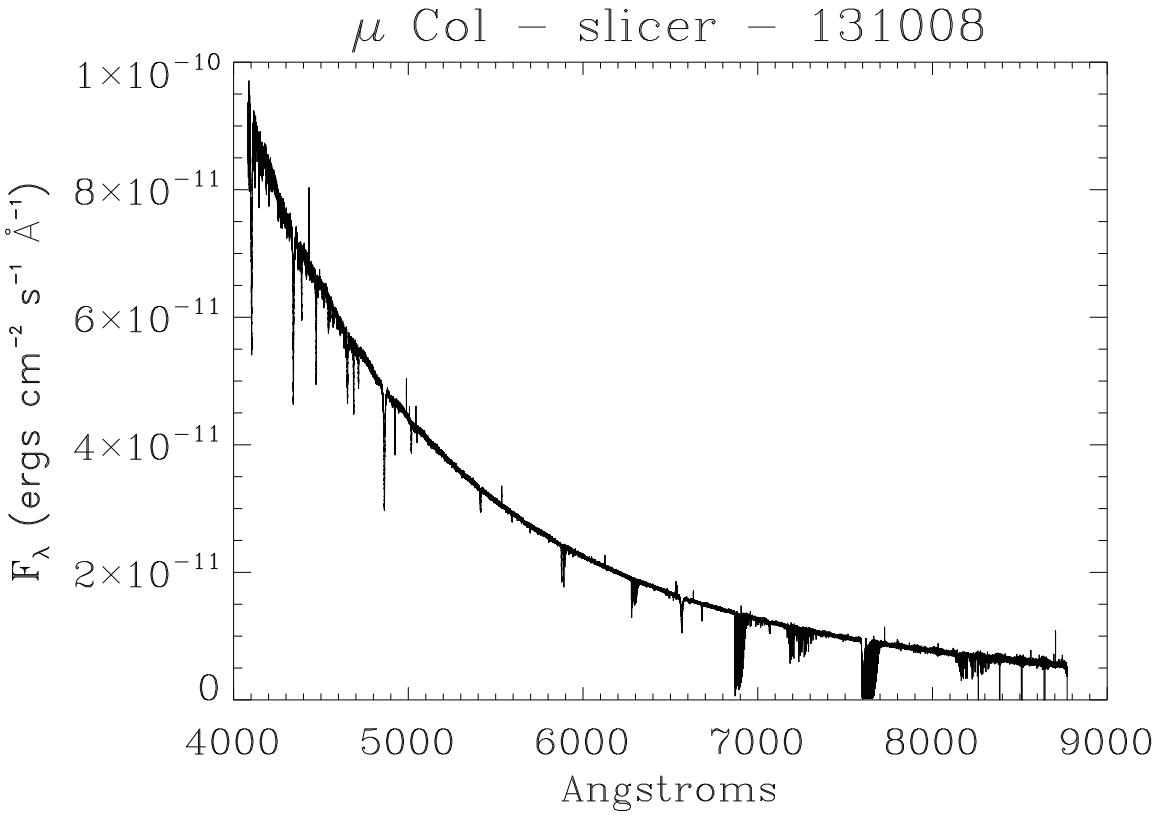

Figure 10: The flux-calibrated slicer spectrum of μ Col (image **chi131008.1140**).

Balmer lines. The conversion (F_λ/count) is saved in **fluxcal_fiber.sav** or **slfluxcal_fiber.sav** in the *chirondata/cal* directory.

There are issues with the calibration near the telluric A and B band heads.

In order to make your own master flux calibration file, you must run *ch_reduce*,/noproc on the flux calibrator. Then run *ch_mkfluxcal*. Specify the observing mode, data, and file with the MODE, DATE, and REC keywords. You will need to change the defaults.

The procedure *ch_calflux* is used to convert the counts spectrum to a flux spectrum. To save this to disk, use *ch_xupdate,flux=1*. The **xchi*.sav** and **xchi*.fits** files are updated. The array in the fits file is expanded. *Rd_Chiron* extracts this as d.f in the d structure.

Note that spectroscopic flux calibration is predicated on the assumptions that both the cali-

Table 7: **Ch_Splice Output Structure**

Tag	Type	Size	Description
W	DOUBLE	Array[*xlen*, N_{ord}]	xchi 2-D wavelength vector
S	DOUBLE	Array[*xlen*, N_{ord}]	xchi 2-D counts vector
E	DOUBLE	Array[*xlen*, N_{ord}]	xchi 2-D signal-to-noise vector
F	DOUBLE	Array[*xlen*, N_{ord}]	xchi 2-D flux vector
H	STRING	Array[]	fits header
W1	DOUBLE	Array[*xlen2*]	spliced 1-D wavelength vector
F1	DOUBLE	Array[*xlen2*]	spliced 1-D flux vector
E1	DOUBLE	Array[*xlen2*]	spliced 1-D signal-to-noise vector
DQ	DOUBLE	Array[*xlen2*]	spliced 1-D data quality vector
SPLICE	DOUBLE	Array[2(N_{ord})-1]	splice points
SKY	FLOAT	0.00000	sky spectrum (not currently used)

brator and the target are observed under photometric conditions, and with equal slit losses. This is often not the case.

Order Splicing: Splicing of the individual orders is accomplished by the *ch_splice* function, called as *z=ch_splice(xfile)*, where *xfile* is the **xchi*.fits** file name or number. *z* is an expanded structure described in Table 7. The output is a save file named **object_YYMMDD.xxxx.sav**, where *object* is from the fits header (with all spaces removed).

The 1-dimensional wavelength vector is linear, with a bin size equal to the smallest in z.w, so that no resolution is lost. The vector length *xlen2* is about 82,000 points in fiber mode and about 322,000 points in slicer mode. The flux and signal-to-noise vectors are interpolated to this linear wavelength scale. The method of splicing is either to do a straight sum (keyword *sum*), to cut by the signal-to-noise vector (keyword *cut*, or to weight by the signal-to-noise vector (default).

When the data are weighed by the errors (signal/signal-to-noise), all negative points are excluded as unphysical.

Because the splice regions are at the ends of the orders, they tend to have low S/N. The file **chirondata/cal/ch_deftrims.dat** lists the empirically-determined "best" cuts, based on visual inspection of the μ Col orders. You can change these with the *trim* keyword, which is added to the defaults (subtracted from the RHS) . *trim* can be be a scalar, a 2-element vector (left, right), or a full (2xN_{ord}) vector.

Setting the *scale* keyword will perform a scaling of the two spectra in the overlap region. This should not be necessary, since the flux calibration serves the same purpose. Furthermore,

in regions where the flux calibration may be suspect (e.g., the edges of strong lines, or the terrestrial A and B bandheads), this may introduce an unwanted shift in the flux levels.

By retaining all *xlen* points in the orders, interorder gaps are eliminated through order 69 (8260Å) when using the default order trims). The user can override the number of points retained for splicing by specifying the *trim* or by editing **ch_deftrims.dat**.

The flux calibration and the order splicing, as well as checking and updating the wavelength solution, are handled by the *ch_postproc* procedure.

5.5 Multiple Spectra

Cosmic ray rejection is simpler, and more robust, when you have two or more spectra of an object obtained on the same night under the same conditions. The routine *ch_reduce* also handles multiple spectra of the same target.

In *ch_reduce*, setting the *do2* or *do3* keywords will result in 2 or 3 consecutive images being coadded prior to extraction. Setting *file* to an N element array has the same effect for non-consecutively numbered files. Currently the code supports N up to 5.

With image pairs, cosmic ray rejection is handled by searching for excursions in the difference image that exceed a multiple (set by the keyword *nsig*) of the expected variance. With 3 or more images, the coadded image is the median at each point. After the coaddition, *ch_reduce* runs as for a single image, with the exception that the output file names are numbered 9xxx rather than xxxx, where xxxx is the number of the first file.

See Figure 21 for an example of a coadded pair of deep exposures.

There may be problems co-adding high S/N pairs or triads with different exposure times, or which differ in instrumental throughput due to variable transparency of the sky. This is because the files are co-added prior to background subtraction.

5.6 Ancillary Software

In almost all cases, typing *procedure,/help* will bring up brief on-line help.

ch_calstatus: check for the existence of calibration data.

ch_sat: identify saturated pixels in **chi*.fits** image.

ch_status: check for unreduced data.

ch_xy: convert between pixel and order/wavelength coordinates.

comp_chx: compare various extraction methods.

plch: quick plot of 1-dimensional *Chiron* spectra

rd_chiron: read fits file, and convert to an IDL structure. Works for both **achi*.fits** and **xchi*.fits** files. Use the *xfiles* keyword to read a **xchi*.fits** file if both types exist.

5.7 Master Calibration Files

The following files are in **chirondata/cal**:

chiron_master_flats.sav A flat spectrum. It is advisable not to use this, but rather to extract the flat on each individual night and use the local **flats_YYMMDD.sav** file.

fluxcal_fiber.sav Flux calibration for the fiber mode spectra.

chiron_master_trace.sav Traces. This is used by default unless *mktrace* is specified in *ch_cals*.

chiron_master_wcal.sav The master wavelength calibration file which is migrated to and tweaked for other nights.

ch_deftrims.dat Default number of pixels to be trimmed from the orders prior to splicing.

The procedure *ch_cals* writes the files specified in table 1 into the **YYMMDD_wcal** directories.

5.8 Run Times

All run times refer to a Linux desktop running CentOS 6.7. The hardware is an Intel Core Duo CPU clocking at 3 Ghz, with 3.8 Gb of memory. The IDL version is 8.1.

Full calibration of a single night requires about 15 seconds for the fiber daya, and about 3 times as long for slicer data. However, enabling Gaussian extractions in fiber mode increases the runtime to about 19 minutes.

Boxcar extraction and post-processing of an image requires less than one minute.

Extraction and calibration of a spectrum, including the Gaussian extraction, requires about 20-25 minutes for high S/N spectra, and up to 50 minutes for noisier spectra. The (lack of) speed is mostly attributable to my using *mpfitfun* to fit 12 free parameters to 1028 slices of the spectrum in each of N_{ord} orders. This can probably be accelerated.

6 Examples

Here I present a few examples comparing my reductions with the Yale reductions. In all plots my reductions are in black. Red ticks at the bottom of the plot indicate pixels flagged as bad.

Figures 11 through 15 are 1800 second integrations taken of N Sco 2015 on 28 or 29 July 2015. The V mag was 15.0 at this time.

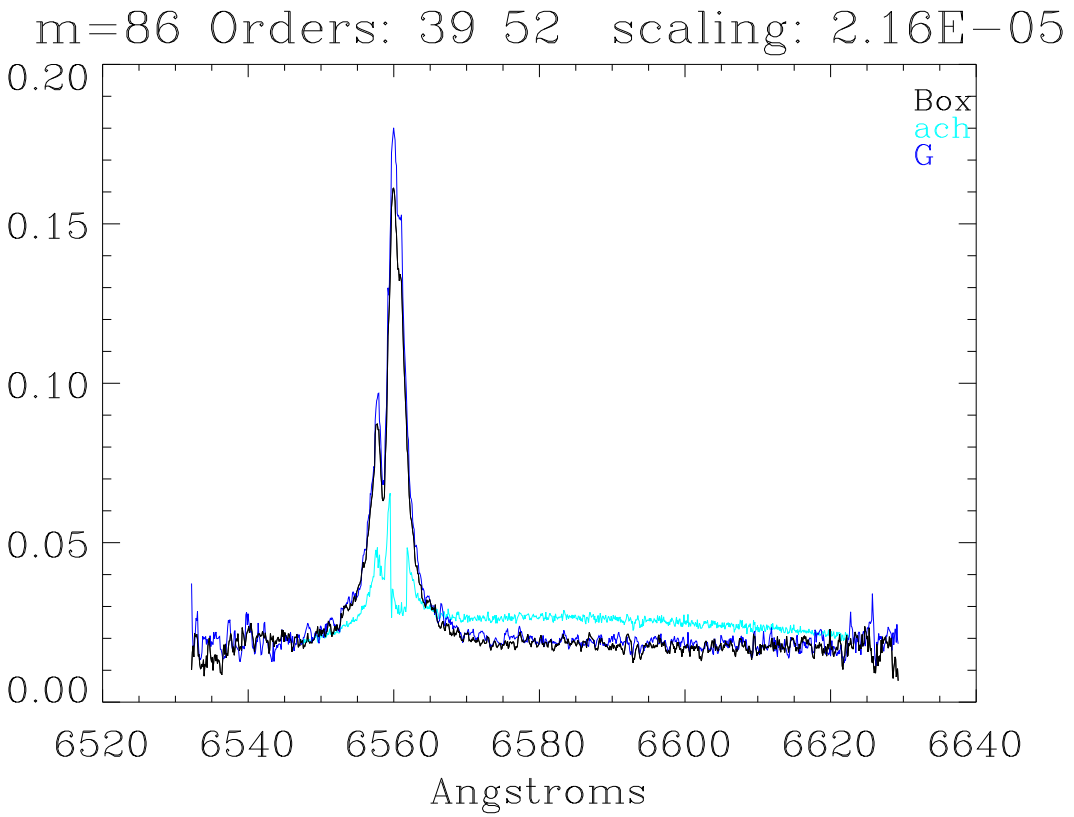

Figure 11: A comparison of the boxcar extraction (black), Gaussian extraction (dark blue) and the Yale extraction (aqua) for the Hα of Nova Sco 2015 (image **chi150728.1124**). The Yale extraction is scaled so the medians match. Note that the central peak of the Hα line is missing in the Yale extractions. It has apparently been flagged as a cosmic ray or some other type of defect. In reality the top of the line is not saturated.

Figure 11 shows the effect of the cosmic ray detection algorithm on the peak of the Hα emission line.

Figures 12 and 13 show the region of the sodium D lines, and illustrate the consequences of subtracting the instrumental background.

Figures 16 through 18 compare slicer-mode extractions. The target is η Car, which has lots of fairly narrow emission lines. The comparison is with the Yale-extracted spectra after I have flux-calibrated and spliced the orders. The absolute fluxes should be ignored; the spectra are scaled by their respective medians. Figure 16 is a region dominated by emission lines; figure 17 shows the Na D region, which is dominated by deep absorption. These figures how that while the overall spectra are similar, there are artifacts attributable to idiosyncracies of the reduction processes. The wavelength scales are not identical. Cosmic ray rejection is not identical. Sharp features are dealt with differently. The two schemes agree well for low-contrast spectral features.

Figures 19 through 20 are of V5668 Sgr (N Sgr 2015b). At this time the novae was near the minimum of its dust dip, but was still reasonably bright, at V=12.5. This is an 1800 second integration.

Figure 21 shows the quality of spectrum one can get on a faint object (V745 Sco at $R > 16$). It also illustrates the quality of the order splicing.

Finally, figure 22 shows a series of slicer-mode spectra taken after the reopening/refurbishment in July/August 2017. These spectra show the growth of the Hα emission line in the very slow nova N Sct 2017 (ASASSN-17hx).

7 Caveats

The code was developed under IDL version 8.1, and in principle will run under version 7. It does not use widgets or object graphics. It does require the IDL Astronomy User's Library[8]. Note that some of the procedures have the same names as built in IDL routines, including *mean* and *gaussfit*. Originally I did this to enhance the functionality or simplify the calls, so they were simple drop-ins. Not sure of that anymore[9]. So when you add this library to your IDL_PATH, consider putting it first.

The Gaussian-extraction part of the code is slow. For now Gaussian extraction is turned off by default in *ch_reduce* and *ch_cals*.

[8] http://idlastro.gsfc.nasa.gov/

[9] Yes, this is bad programming practice. But it would be a lot of effort to edit 30 years worth of homegrown code. And I'm pretty sure I wrote my *mean.pro* before RSI did.

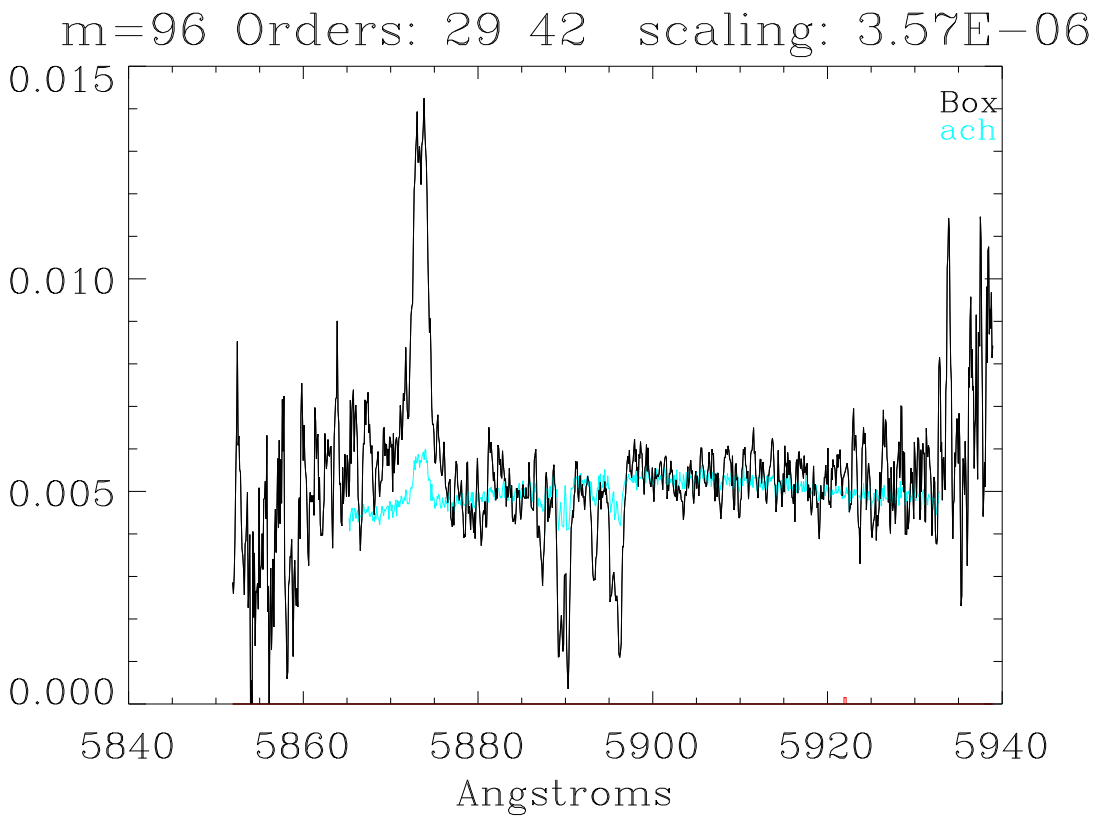

Figure 12: A comparison of the boxcar extraction (black) with the Yale extraction (aqua) for the sodium D line region of Nova Sco 2015 (image **chi150729.1124**). The Yale extraction is scaled so the medians match. Note that the line strengths are much weaker in the Yale reduction, while the S/N is higher. This suggests that the background has not been subtracted in the Yale reductions (see figure 13). The emission line is He I λ5876. Multiple velocity components are visible in the Na D_1 and D_2 lines. The low velocity components are galactic foreground; the blue-shifted absorption lines may be ejecta from the nova.

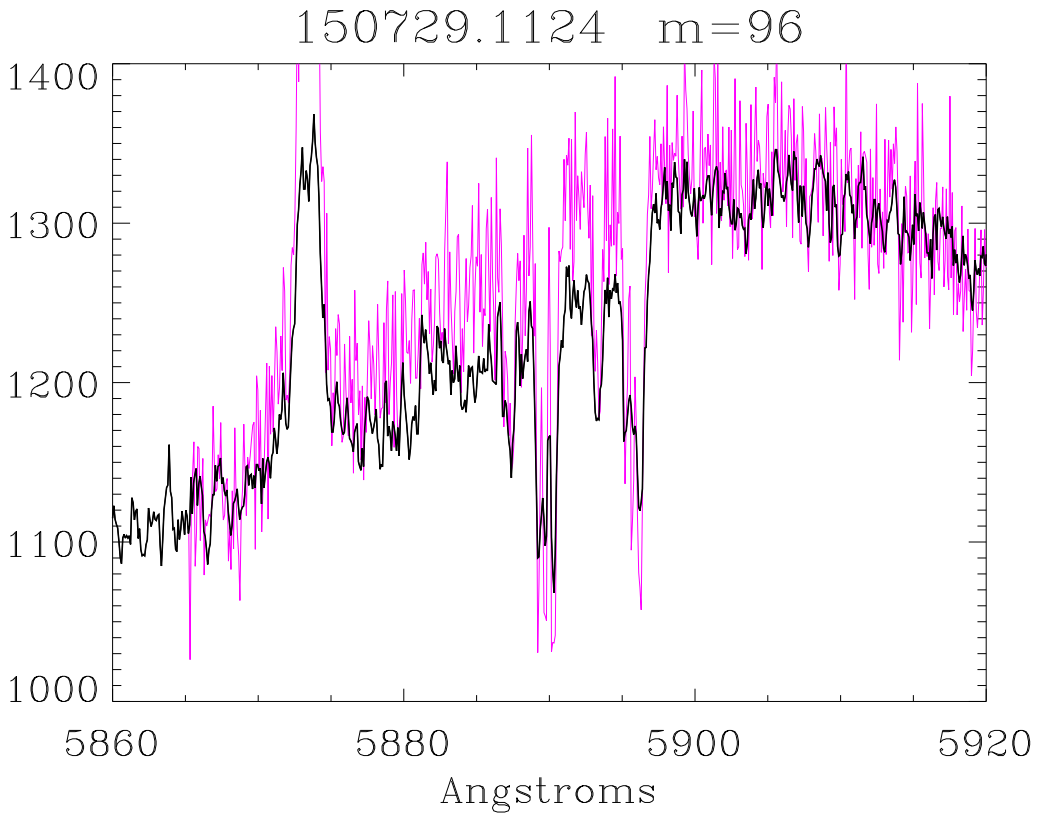

Figure 13: This is the same data as shown in figure 12, except that the data (black) are not flattened, and the background has not been subtracted. This provides a reasonably good match to the Yale reductions (magenta).

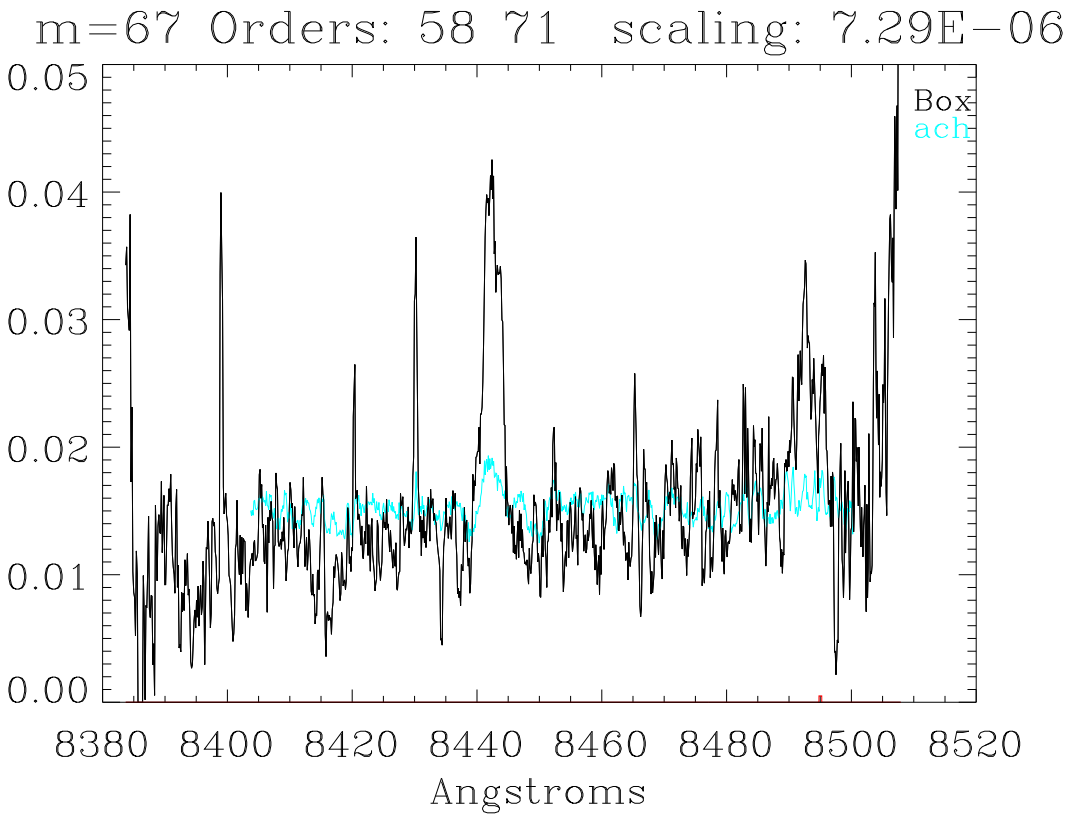

Figure 14: Order 67, showing strong emission from the λ8498 component of the Ca II IR triplet. The line is not evident in the Yale reductions. The apparent strengths of the λ8446Å O I line are also very different.

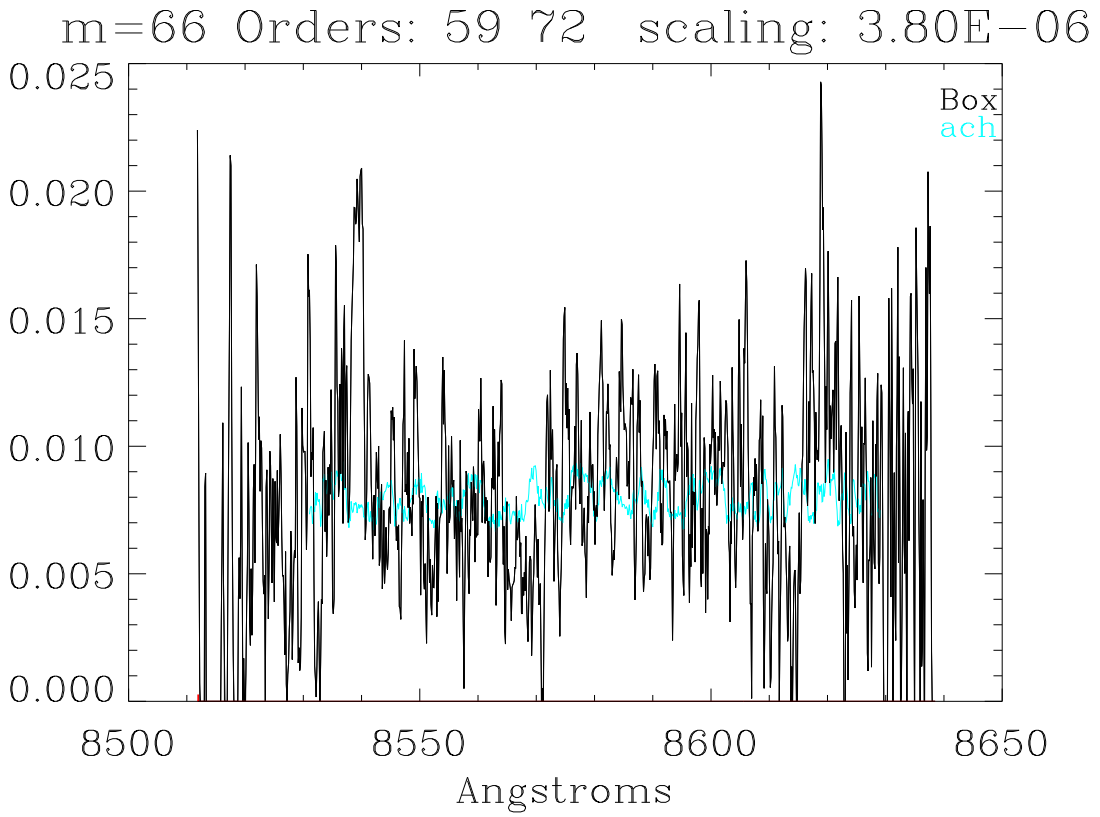

Figure 15: Order 66, showing strong emission from the λ8542 component of the Ca II IR triplet. As in figure 14, the line is not evident in the Yale reductions.

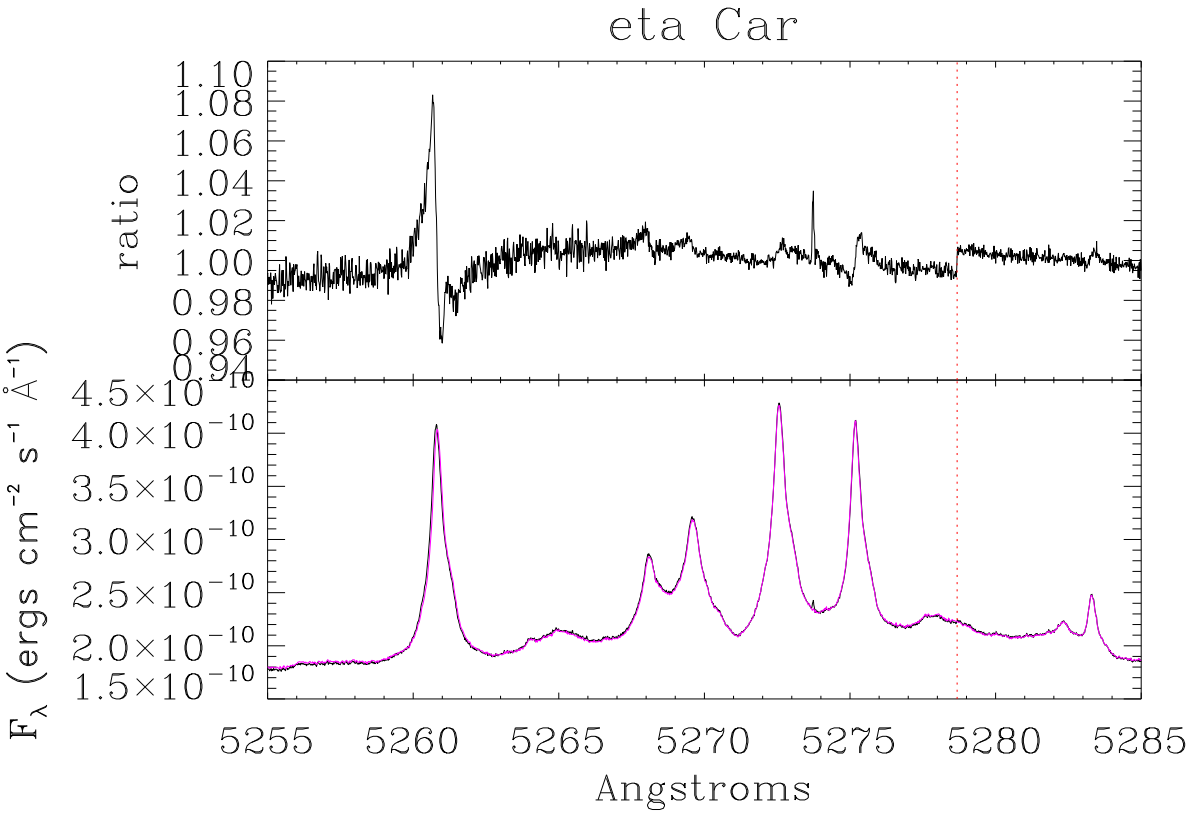

Figure 16: A region dominated by emission lines (mostly Fe III). In the lower plot, the black trace is from the new reductions while the magenta trace is the Yale extraction after flux calibration and order splicing. The upper plot shows the ratio of the two. The dotted vertical line shows an order splice. The upper plot shows 3 artifacts. There are wavelength offsets in the λ5261Å and 5275Å lines, but the senses are different, suggesting that one wavelength scale is stretched relative to the other. The positive excursion in the ratio at 5274Å is a cosmic ray or hot pixel not flagged in my reduction scheme (it is not designed to work well in highly non-linear regions). The 1% step at the order splice at 5279Å is in the new reduction scheme.

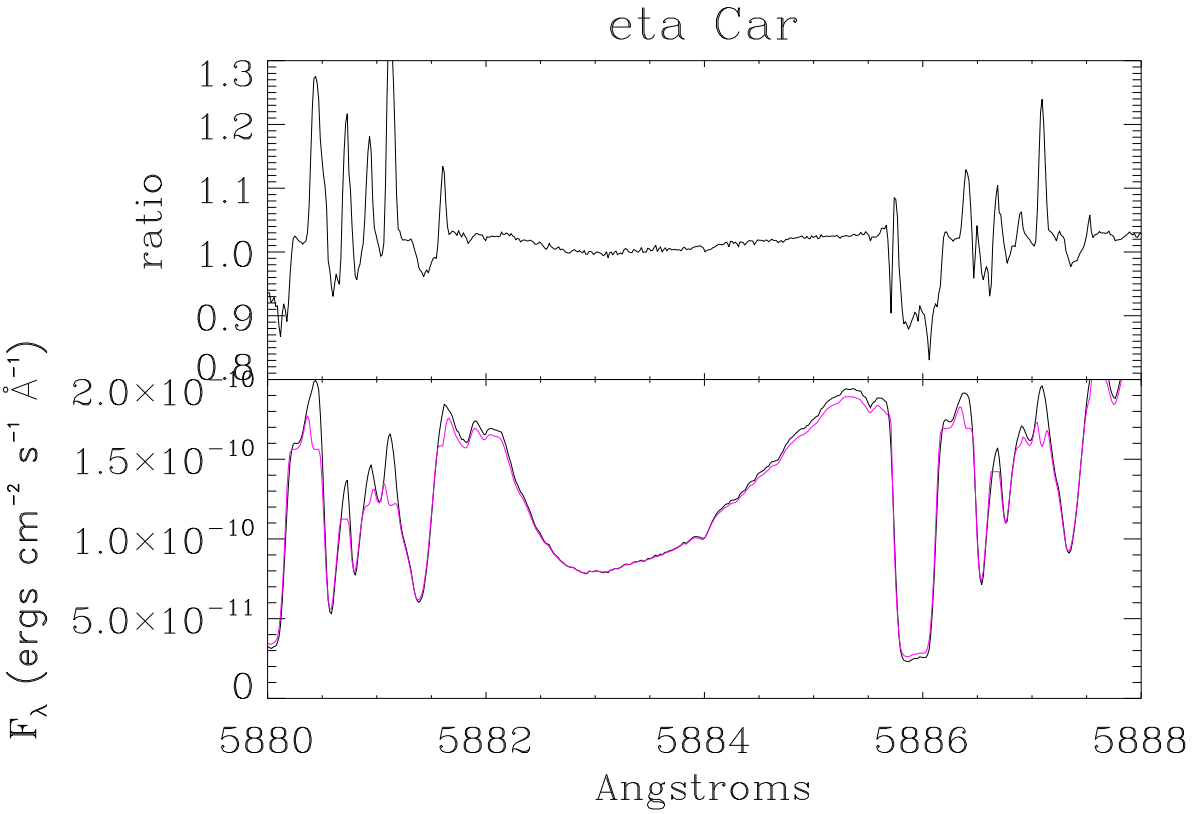

Figure 17: A region on the blue side of the broad Na I emission line. Setup is as in figure 16. The deep absorption line (presumably due to discrete Na I absorption at -200 km/s in the homunculus) is deeper in my reductions, probably because of the global background subtraction. The narrow peaks between absorption lines (especially near 5881Å) are sharper in my extractions

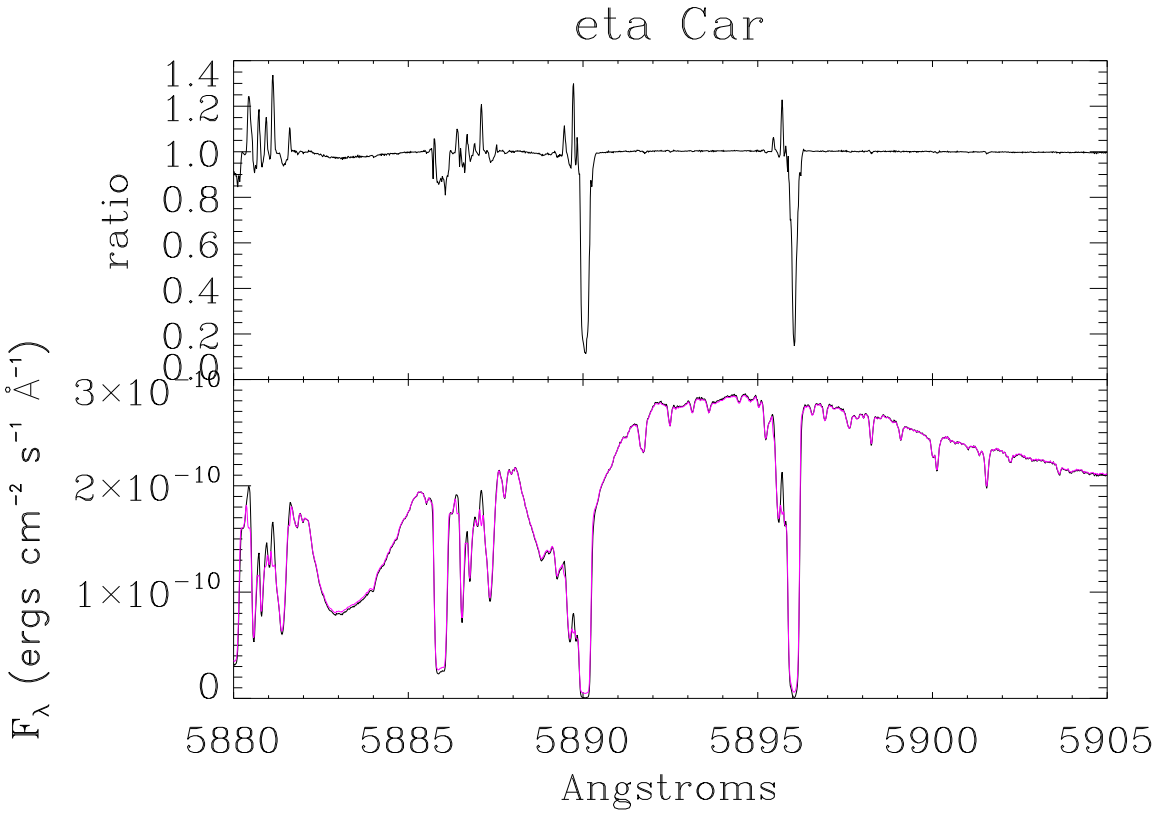

Figure 18: The NaD line region. Setup is as in figure 16. The low velocity Na D lines are undersubtracted in the Yale extractions. My reductions return sharper features on the blue sides of the Na D absorption lines. For low contrast lines (e.g., in the 5896-5905Å region and between the Na D lines), the two schemes agree to better than 1%.

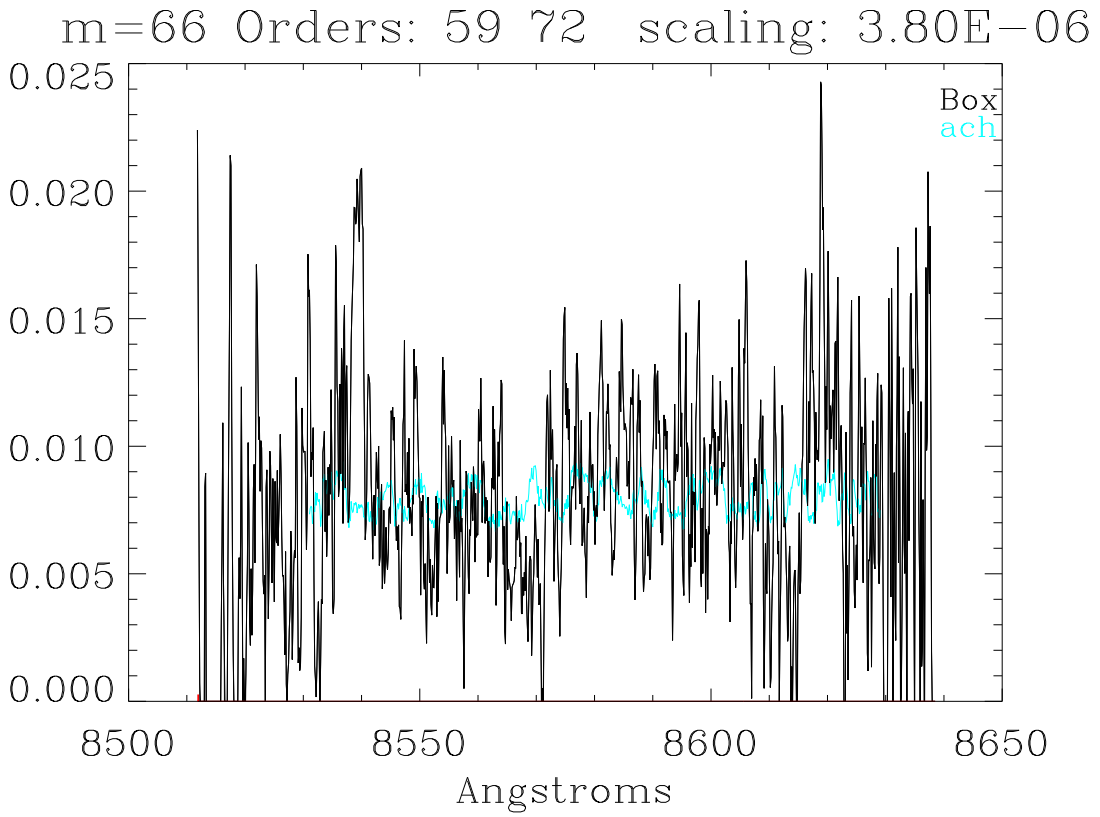

Figure 19: V5668 Sgr in its dust dip. Order 66, showing strong emission from the λ8542 component of the Ca II IR triplet. As in figure 14, the line is not evident in the Yale reductions.

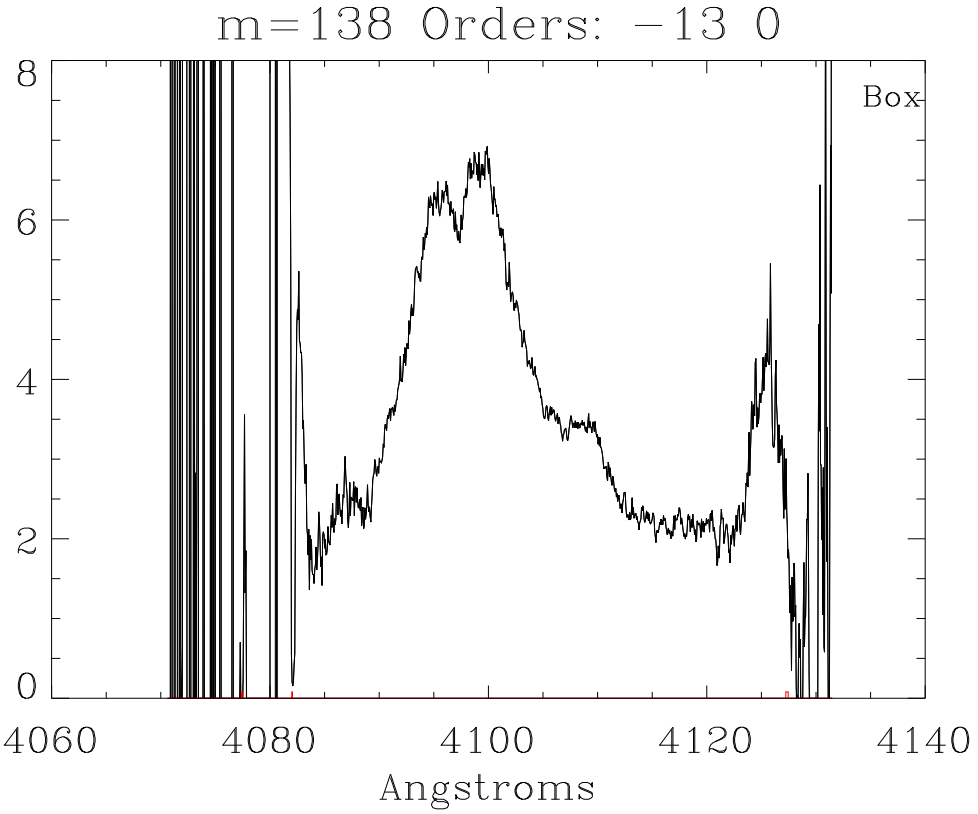

Figure 20: The Hδ λ4100 line in V5668 Sgr. The other line is probably Fe II λ4128 (multiplet 27). This is as blue as Chiron goes. All 1028 pixels are plotted; nothing has been masked. There is not much sensitivity at the ends of the order.

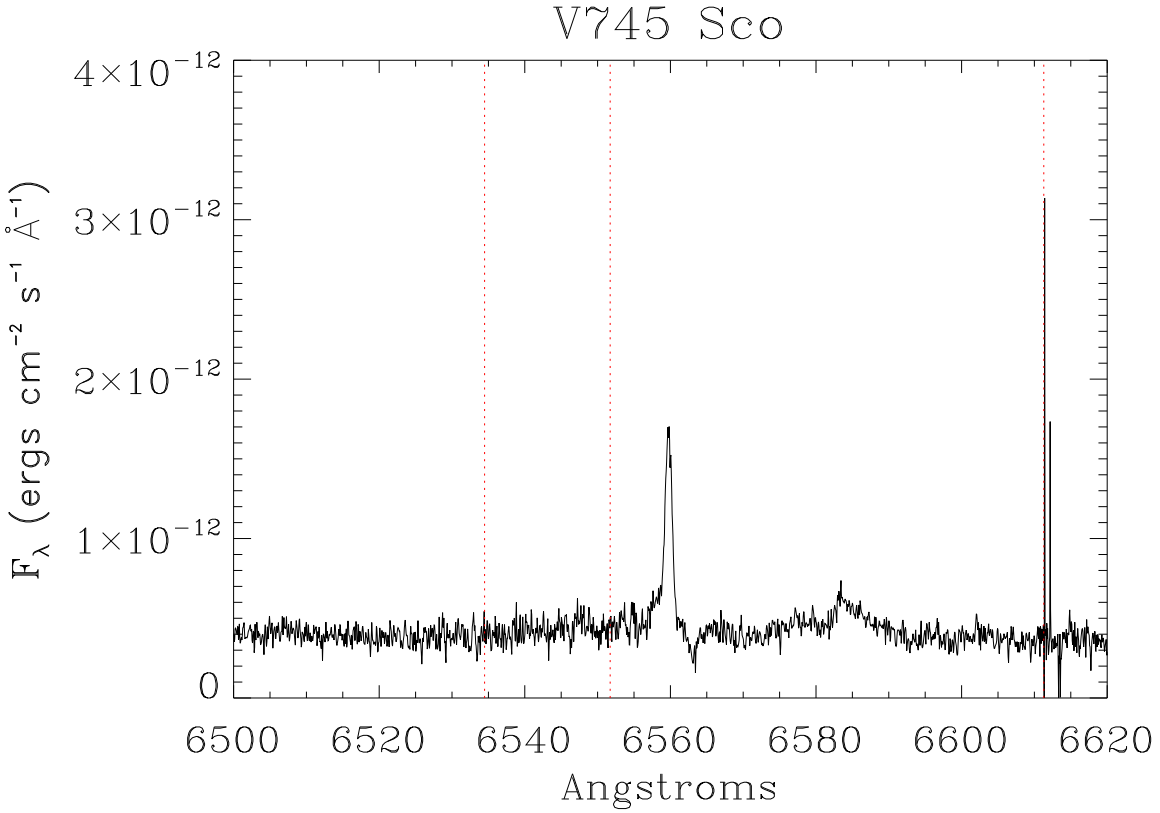

Figure 21: The Hα region of V745 Sco on 150603. This is the sum of two 1800 second integrations, reduced using *ch_reduce*. The R mag at the time of observation was about 16.2. The dotted red vertical lines mark the spliced regions. No background has been subtracted; the data are unsmoothed. The default trims have been expanded by 10 pixels. The high points are due to low counts at the edge of the detector rather than to cosmic rays. The narrow emission is Hα; the source of the broad emission near 6585Å is not currently known. No sky has been subtracted; much of the continuum and the 6563Å absorption may be from the night sky.

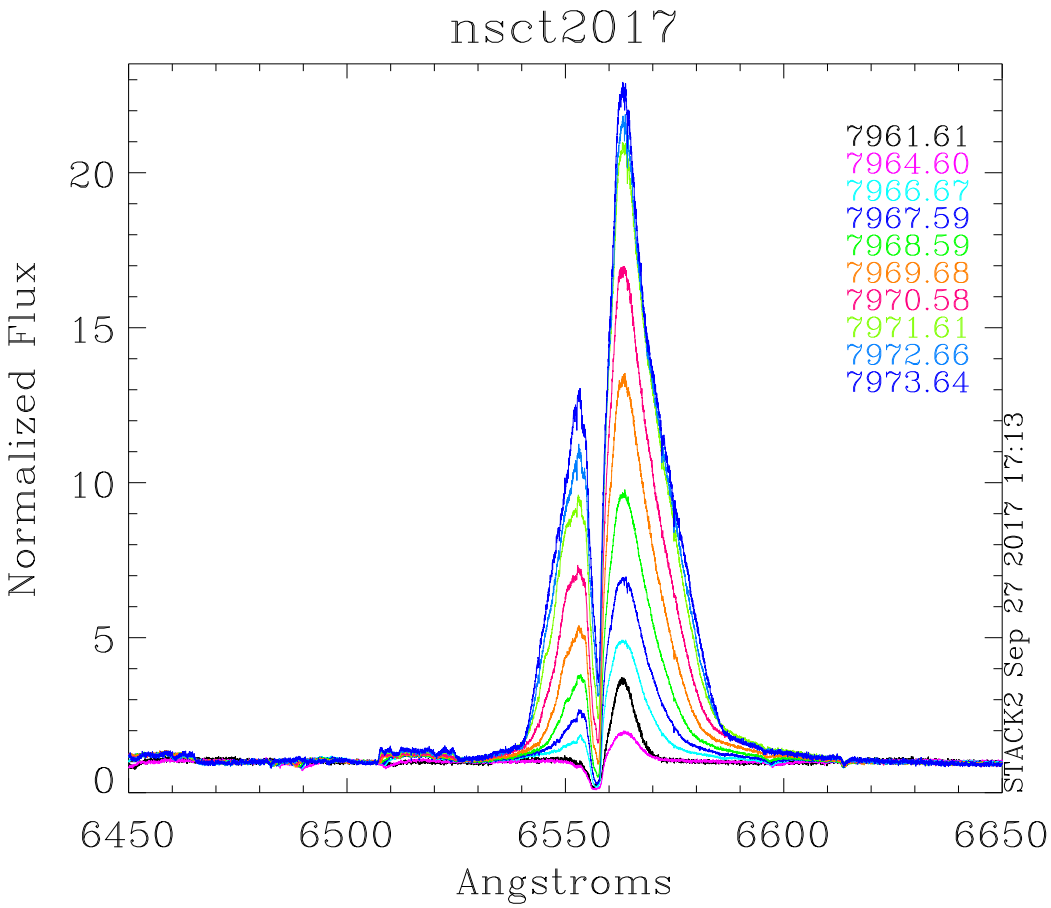

Figure 22: Slicer-mode spectra of nova Sct 2017 on 10 nights between 26 July and 7 August 2017, taken during the recommissioning of the spectrograph. Fluxes are normalized to the 6470-6507Å continuum. After an initial dip from days 7961 to 7964, the line grew steadily stronger and broader. The fuzz at 6456 and 6517Å is the emerging broad and flat-topped Fe II emission. The 6613Å absorption is a diffuse interstellar band.

While the wavelengths match up well with those of the Yale reductions, I have not tested the fidelity of the solutions. I have not done any rigorous testing of the stability of the wavelength solution. Use this code for precise radial velocity work with caution.

Although this code has run on over 1000 images from 572 nights without breaking, there is no guarantee that there are no bugs left, or that all the analysis is being done correctly[10]. The user always has the final responsibility for verifying data quality. Bugs or unexpected features may be brought to the author's attention at frederick.walter@stonybrook.edu

8 The Software

The procedures and the master calibration files are available in two tar files. Open
http://www.astro.sunysb.edu/fwalter/SMARTS/NovaAtlas/ch_reduce/ch_reduce.html
in your browser. You will find links to this documentation and to ch_pros.tar.gz (the procedures) and ch_calibs.tar.gz (the master calibrations).

9 Coming Later?

Possible augmentations include:

- Sky subtraction capabilities, using actual spectra of the night sky.
- Testing of optimal extraction codes. At present the Gaussian fit is just that - a Gaussian fit (ignoring data previously flagged as bad). It is possible to flag significant deviations in the data against the model, and refit excluding those points. If properly tuned, this can remove cosmic rays otherwise missed.

10 Summary

This reduction package provides, for both fiber and slicer mode observations, better quality spectral extractions for faint targets than those provided by default. Thirteen more orders, from 4085Å through 4510Å, are extracted, and all the points along each spectral order are available. Uncertainties (more precisely, the signal-to-noise ratio) are tracked for each point. The extraction does a better job subtracting the background than does the standard reductions. The extracted spectra, when divided by the flats, are flat. This simplifies the problems of flux calibration and order splicing.

For slicer mode observations, the 13 bluest orders are also extracted. The interorder background is subtracted globally.

[10]No process can ever be made completely foolproof, because fools are so ingenious.

The output data products are an array of flux-calibrated orders and a single spliced spectrum with no gaps shortward of 8260Å. The data are stored in both fits format and as IDL save files.

This code may enable more kinds of scientifically-useful observations with the *Chiron* spectrograph. But it is up to the astronomer to understand their data and the limitations of the instrument, the data, and the extraction and calibration tools used.

The IDL procedures and the master calibration files are available through my nova web page, http:/www/astro.sunysb.edh/fwalter/SMARTS/NovaAtlas/ .

11 Acknowledgments

I thank the former Provost of Stony Brook University, Dr. Dennis Assanis, for supporting my participation in SMARTS. I thank the SMARTS Chiron scheduler, Emily MacPherson, for service above and beyond the call of duty in scheduling Chiron observations of novae in a timely fashion. I thank Andrei Tokovinin for a careful reading of and comments on a draft of this document. I thank various experts, among them U. Munari, S. Shore, and R. Williams, for looking critically at and questioning some of the spectra I tried to feed them.

Todd Henry challenged me to extend the extractions to the slicer-mode, in return for some engineering data (which looks pretty good scientifically).

Not a penny of NSF money has been expended on this project.

12 References

Markwardt, C. https://www.physics.wisc.edu/∼craigm/idl/fitting.html
Pych, W. 2004, PASP, 116,148
Tokovinin, A. et al., 2013, PASP, 125, 1336
Valenti, J. 1999. available at https://github.com/mattgiguere/idlutils/blob/master/thid.pro
van Dokkum, P.G. 2001, PASP 113, 1420